The Canadian Mineralogist
Vol. 35, pp. 1093-1115 (1997)

METAMORPHIC P–T PATHS FROM THE EASTERN FLIN FLON BELT AND KISSEYNEW DOMAIN, SNOW LAKE, MANITOBA*

THOMAS MENARD[1] AND TERENCE M. GORDON

Department of Geology and Geophysics, University of Calgary, Calgary, Alberta T2N 1N4

ABSTRACT

Alteration zones around a volcanogenic Cu–Zn–Au massive sulfide deposit in the Paleoproterozoic Trans-Hudson Orogen at Photo Lake, near Snow Lake, Manitoba, and in the Kisseynew Domain experienced multiple stages of metamorphism and metasomatic alteration during the deformation events. In the Snow Lake area, F_1 produced a chlorite-grade schistosity. During F_2, pressure increased by 1–2 kbar, and temperature increased by 10–50°C, up to approximately 5 kbar and 550°C, at which time most of the F_2 strain occurred, destroying most evidence of S_1. This was followed by a continued temperature increase of 10–20°C. Peak metamorphic, syn-F_2 assemblages in the altered volcanic rocks include staurolite + garnet + biotite, and kyanite + chlorite. F_3 produced a crenulation of S_2, along with minor chloritization at 400–450°C. In alteration zones in the Kisseynew Domain, S_1 is obscure, but garnet grew prior to, during, and after the development of the S_2 fabric, as is the case at Snow Lake. Likewise, metamorphic conditions during F_2 were similar to those at Snow Lake during F_2. However, rocks in the Kisseynew Domain were heated another 100–150°C after growth of the garnet, as shown by the assemblage sillimanite + garnet + biotite and geothermometry. They also acquired a gneissic fabric at or near the thermal peak of metamorphism. Garnet + cordierite assemblages and geobarometry suggest that metamorphic pressures during the thermal peak were similar to those at garnet grade. The final heating event occurred after F_2 deformation, and requires a source of heat localized under the Kisseynew Domain. Likely scenarios include emplacement of plutons in and under the Kisseynew Domain during F_2.

Keywords: Snow Lake, Trans-Hudson Orogen, Kisseynew Domain, metamorphic petrology, P–T paths, Manitoba.

SOMMAIRE

Les zones d'altération entourant un gisement volcanogénique de sulfures massifs à Cu–Zn–Au de la ceinture orogénique paléoprotérozoïque de Trans-Hudson, au lac Photo, près du lac Snow, au Manitoba, et dans le domaine adjacent de Kisseynew, ont subi plusieurs stades de métamorphisme et d'altération métasomatique lors des événements de déformation. Dans la région du lac Snow, F_1 a produit une schistosité dans le champ de stabilité de la chlorite. Au cours de F_2, la pression a augmenté de 1 à 2 kbar, et la température, de 10 à 50°C, jusqu'à un seuil d'environ 5 kbar et 550°C; c'est à ce stade que la plupart de la déformation F_2 a affecté ces roches, oblitérant par le fait même les signes de S_1. Cet épisode a été suivi par une augmentation continue en température de 10 à 20°C. Parmi les assemblages typiques du paroxysme métamorphique, formés pendant F_2 dans les roches volcaniques altérées, figurent les associations staurolite + grenat + biotite, et kyanite + chlorite. F_3 a produit un plissement de S_2, avec une légère chloritisation à 400–450°C. Dans les zones d'altération du domaine de Kisseynew, S_1 est obscur; en revanche, le grenat s'est formé avant, pendant, et après le développement de S_2, tout comme c'était le cas au lac Snow. De même, les conditions du métamorphisme au cours de F_2 étaient semblables à celles dans la région du lac Snow. Par contre, les roches du domaine de Kisseynew ont été réchauffées environ 100 à 150°C après la croissance du grenat, comme le témoignent les assemblages à sillimanite + grenat + biotite et la géothermométrie. Ces roches ont de plus acquis une gneissosité lors du maximum thermique. Les assemblages à grenat + cordiérite et la géobarométrie font penser que la pression atteinte lors du maximum thermique ressemblait à celle dans le faciès à grenat. L'événement thermique final a eu lieu après la déformation F_2, et requiert une source de chaleur en dessous du domaine de Kisseynew. Il est probable que la mise en place de plutons dans et sous ce socle au cours de F_2 en soit la cause.

(Traduit par la Rédaction)

Mots-clés: lac Snow, ceinture orogénique Trans-Hudson, domaine de Kisseynew, pétrologie métamorphique, tracé P–T, Manitoba.

*LITHOPROBE publication number 1001.

[1] *E-mail address*: tmenard@geo.ucalgary.ca

INTRODUCTION

The Flin Flon greenstone belt and the Kisseynew gneiss domain in northern Manitoba (Fig. 1) have been the focus of recent lithological and structural mapping, geochronology, geochemistry, and geophysics undertaken during collaborative efforts by geologists involved with the Lithoprobe Trans-Hudson Orogen Transect, the Geological Survey of Canada's Shield Margin Project, and the Manitoba Energy and Mines. The resulting explosion of new data and interpretations provides an ideal framework for studies of metamorphic petrology focused on understanding the tectonic history of the region. In this paper, we present detailed

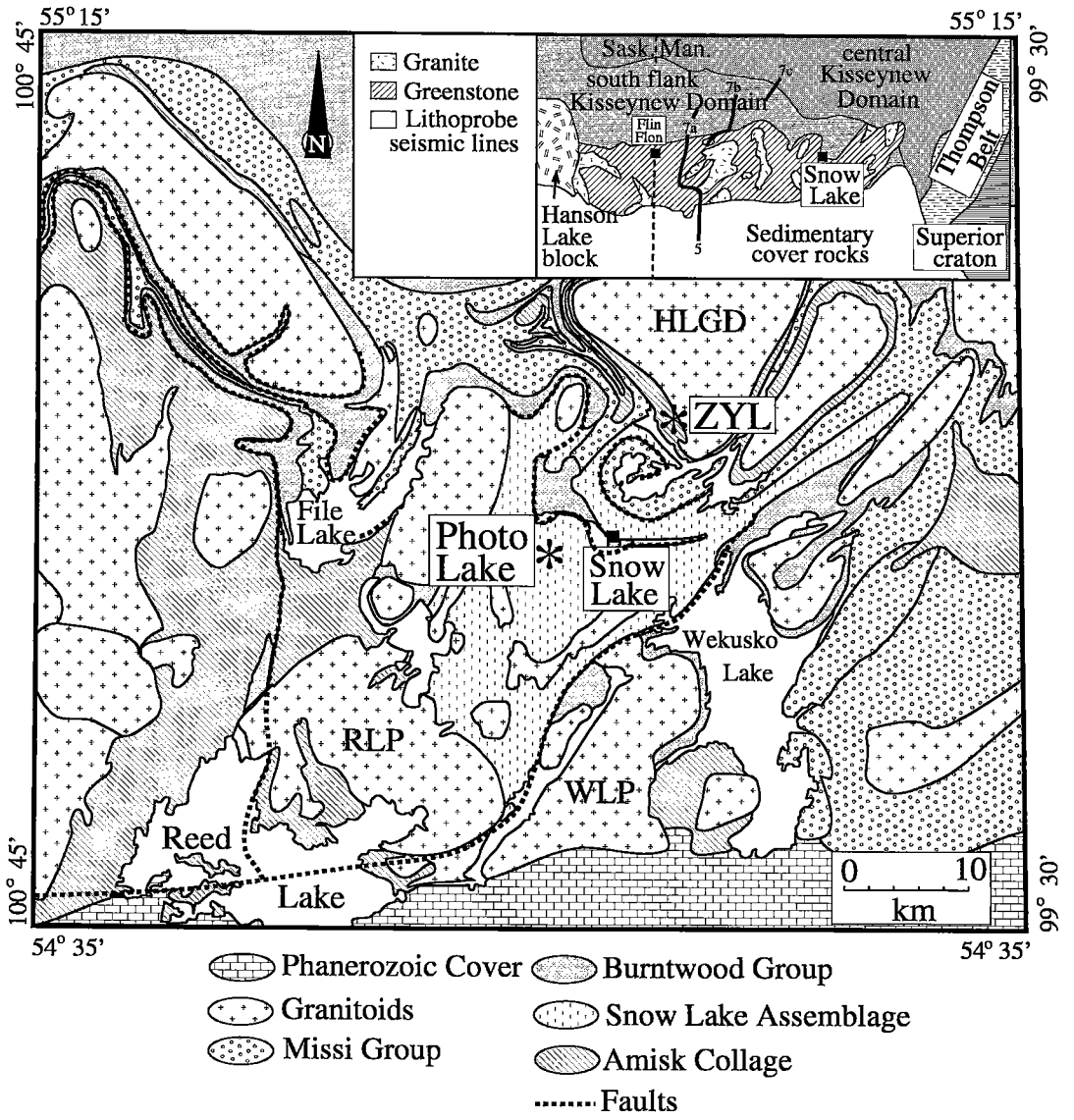

FIG. 1. Geology of the Snow Lake area, with location of samples marked by asterisks (Bailes 1996). Inset shows location of Lithoprobe seismic lines (Lucas *et al.* 1994, Kraus & Williams 1993). In the Snow Lake area, the Kisseynew Domain is interleaved with the Flin Flon Belt along the marked faults. HLGD: Herblet Lake gneiss dome, RLP: Reed Lake pluton, WLP: Wekusko Lake pluton.

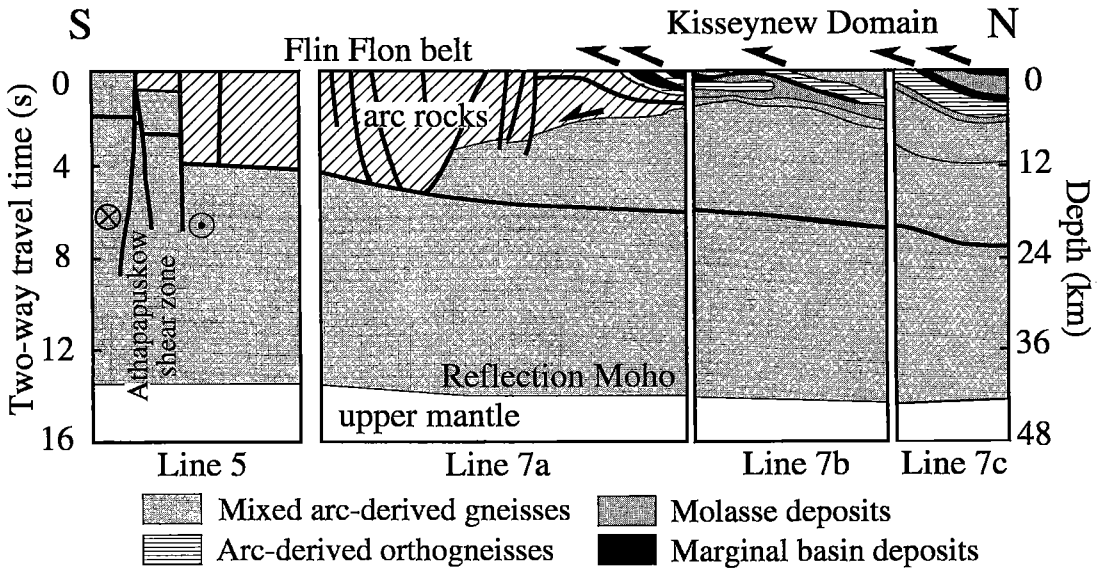

FIG. 2. Interpretation of Lithoprobe seismic data of lines 5 and 7 (Lucas *et al.* 1994). Thrusts and isoclinal folds were produced during F_1, and again during F_2 (illustrated) near the thermal peak of metamorphism.

results on the metamorphic petrology of a few samples from the Flin Flon Belt at Snow Lake and from the Kisseynew Domain to the north, and use those results to interpret the regional tectonic evolution.

REGIONAL SETTING

The Snow Lake area straddles the boundary between the Flin Flon greenstone belt to the south and the Kisseynew gneiss domain to the north (Fig. 1). Volcanic rocks of the Flin Flon belt at Snow Lake are mainly of island-arc affinity, with minor units of ocean-floor rocks (Bailes 1988, Stern *et al.* 1995, Bailes & Galley 1996). The Kisseynew gneisses at Snow Lake consist mainly of the Burntwood Group metaturbidites and correlative Missi Group fluvial-deltaic metasandstones (Froese & Moore 1980).

The central Kisseynew Domain experienced uniform peak metamorphism at *ca.* 750°C and 5–6 kbar (Bailes & McRitchie 1978, Gordon 1989, Gordon *et al.* 1994). Inferred peak metamorphic temperatures decrease to chlorite grade south of Snow Lake, although inferred pressures remain nearly constant at 4–6 kbar (Bailes & McRitchie 1978, Kraus & Menard 1997). Thus the Kisseynew Domain had a markedly higher and more uniform geothermal gradient than the Flin Flon Belt during the Trans-Hudson Orogeny (Bailes & McRitchie 1978, Gordon *et al.* 1990, Jungwirth & Gordon 1993, Digel & Gordon 1995, Kraus & Menard 1997).

Lithoprobe seismic reflection lines 5 and 7, which cross the Flin Flon Belt and the southern part of the Kisseynew Domain (Fig. 1), have been interpreted by Lucas *et al.* (1994) to show isoclinal folding and thrust faulting of the Kisseynew Domain southward over the Flin Flon Belt (Fig. 2). We interpret this to be our F_2 event at Snow Lake. Figure 2 was constructed from seismic data, and hence displays fewer and different units than the geological map in Figure 1. The thrust sheets and fault slices have an apparent thickness of *ca.* 4 km below the present erosion-surface. However, the total thickness of overthrusting is ambiguous because of the effects of erosion and the possibility of stacking of repeated thrusts and isoclinal fold sheets.

GEOLOGY OF SNOW LAKE

Stratigraphy and structure

Stratigraphic units and F_1–F_3 structures in the Snow Lake area have recently been mapped by Bailes (1996), Bailes & Galley (1992), Bailes & Simms (1994), and Kraus & Williams (1993, 1994, 1995). Volcanic rocks and synvolcanic tonalites were emplaced at approximately 1.89 Ga (Machado & David 1992, David *et al.* 1996). Sedimentary rocks of the Missi Group are younger than 1845 Ma (Ansdell *et al.* 1992) and broadly correlative with sedimentary rocks of the Burntwood Group in the Kisseynew Domain (David *et al.* 1996).

At Snow Lake, rocks of the Kisseynew Domain and Flin Flon Belt were structurally interleaved during F_1 and F_2 deformation, producing a zone that is characteristic of the "south flank" of the Kisseynew Domain (Kraus & Williams 1994). F_1 produced tight to

isoclinal folds and a muscovite cleavage in the Snow Lake area (Froese & Moore 1980, Kraus & Williams 1994) prior to emplacement of the 1840–1834 Ma Wekusko granite (Gordon *et al.* 1990, David *et al.* 1996), which cross-cuts F_1 folds (Bailes 1992, Kraus & Williams 1995). F_2 folds at Snow Lake area are displayed in map relations and manifest as a crenulation cleavage that wraps around the porphyroblasts formed at the peak of metamorphism (Kraus & Williams 1994). Metamorphism during F_2 has been dated at 1810 Ma, based on titanite ages from the Anderson–Stall rhyolite (Machado & David 1992). F_3 produced upright, open folds during retrograde metamorphism at 1800–1790 Ma (Kraus & Williams 1995, Parent *et al.* 1995). F_4 produced east–west-trending folds around gneiss domes in the southern flank of the Kisseynew Domain (Kraus & Williams 1994). Subsequent brittle faults (Bailes & Galley 1992) are associated with minor alteration to pumpellyite (unpubl. data).

Metamorphism

Metamorphism in the Snow Lake area has been the subject of several previous studies (Froese & Gasparrini 1975, Bailes & McRitchie 1978, Hutcheon 1979, Froese & Moore 1980, Trembath 1986, Aggarwal & Nesbitt 1987, Bryndzia & Scott 1987, Bristol & Froese 1989, Zaleski *et al.* 1991, Kraus & Menard 1997). These studies documented isograd reactions and compositions of minerals, and established the general trend of increasing metamorphic grade to the north. Hutcheon (1979) found that the Fe/(Fe + Mg) of silicate minerals in sulfide-bearing samples is lower than in samples without sulfides. Zaleski *et al.* (1991) showed that the assemblage kyanite + biotite + chlorite in the Linda deposit appears as the result of Mg- and F-rich biotite and not of the common isograd reaction St + Chl + Ms + Qtz = Ky + Bt + H_2O. Here and elsewhere, mineral symbols follow Kretz (1983). Rare sillimanite was reported from the Anderson Lake deposit in the Snow Lake area (Aggarwal & Nesbitt 1987), which would suggest that metamorphic conditions were near the kyanite–sillimanite phase boundary at some stage of the metamorphic history.

Metamorphism of alteration zones around volcanogenic massive sulfide deposits in the Snow Lake area involved additional stages of compositional alteration during and after the thermal peak of metamorphism (Menard & Gordon 1995). In several locations across the study area, 5- to 20-m-long sections of diamond-drill core now consist of chlorite schist with variable amounts of plagioclase and other minerals. Minerals preserved in the core of porphyroblasts indicate that the rocks had contained biotite and hornblende and may have been diorite. These features may reflect synmetamorphic flow of fluid focused along faults.

Ore deposits

The Snow Lake area contains numerous volcanogenic massive sulfide deposits and mesothermal gold deposits. Exploration and mining activities in the area provided access to altered volcanic rocks in the Photo Lake Cu–Zn–Au mine, operated by Hudson Bay Exploration & Development Company, and the New Britannia gold mine (formerly the Nor-Acme mine), operated by TVX Gold, Inc., which is the largest known gold deposit in the Trans-Hudson Orogen. The geochemistry of alteration in the volcanogenic massive sulfide (VMS) deposits was studied at the Chisel Lake deposit by Galley *et al.* (1993) and at the Cook Lake deposit by Hodges & Manojlovic (1993).

METHODS

More than 600 samples of rocks from outcrops, diamond-drill core, and underground exposures in mines were collected from the study area. More than 200 samples from the Flin Flon belt and the Kisseynew Domain in the Snow Lake area, and 10 samples from the Kisseynew gneisses were selected for petrographic analysis to provide geographic distribution and a variety of rock types. From these, 20 samples that contain appropriate mineral assemblages and obvious deformation-related fabrics were selected for electron-microprobe analysis at the University of Calgary and the University of Alberta. The program of analyses included spot analyses, using oxides and natural minerals as standards and secondary standards, back-scattered electron imaging, and X-ray maps of the compositions of mineral grains. Thermobarometric estimates were calculated using the following calibrations: garnet + biotite (Kleeman & Reinhardt 1994), garnet + chlorite (Dickenson & Hewitt 1986) with Berman's (1990) garnet model, garnet + plagioclase + biotite + muscovite (Hodges & Crowley 1985, Powell & Holland 1988, Hoisch 1990), and garnet + plagioclase + biotite + quartz (Hoisch 1990). The resulting pressures and temperatures were compared with results from the WebINVEQ thermobarometry program (Gordon 1992, Gordon *et al.* 1994), using thermodynamic data from Berman (1988), as modified in Berman (1991), and activity models for garnet (Berman 1990, Berman & Koziol 1991), amphibole (Mäder *et al.* 1994), biotite (McMullin *et al.* 1991), and plagioclase (Fuhrman & Lindsley 1988).

The sequence of pressures and temperatures experienced by a rock during metamorphism reflects the tectonic processes operating at the time, and can be recorded by the history of metamorphic reactions and compositional zoning of the minerals. The theoretical background for computation of a metamorphic P–T path based on the Gibbs method is given by Spear & Selverstone (1983), and a comprehensive review was

given by Spear (1993). Briefly, calculation of a metamorphic P–T path usually requires that the following be known for a given rock: the history of metamorphic reactions, the assemblage of minerals and their compositions at some time, the pressure and temperature at that time, and the correlation between compositional zoning of two minerals. Uncertainties in the starting pressure, temperature, and some mineral compositions usually propagate into relatively small errors in the shape of the P–T path (Kohn 1993). Instead, the critical factor in constructing a P–T path is the correlation of compositional zoning in the minerals. Precision in the calculated P–T path is usually much better than in paths constructed by thermobarometry. The necessary differential thermodynamic equations can be written without using mineral abundances or the bulk-rock composition. Consequently, metasomatism does not affect the calculated P–T path. Calculations based on the Gibbs method were performed using the computer program of Spear *et al.* (1991) and thermodynamic data from Berman (1988). Thermodynamic data for phase components not listed by Berman (1988) were computed using the method of Kohn *et al.* (1993), with exchange values from Holland (1989) and data for ZnO from Robie *et al.* (1979). Nonideal activity models were used for garnet (Berman 1990), plagioclase (Newton *et al.* 1980), and H_2O (Haar *et al.* 1979). No miscibility gaps in subsolidus plagioclase were observed.

Mineral Assemblages

Samples described from Snow Lake come from metamorphosed alteration zones adjacent to the Photo Lake Cu–Zn–Au VMS deposit, 5 km southwest of the town of Snow Lake, and a possible northern extension of the Chisel Lake VMS deposit, 2 km south of the Photo Lake deposit. Metamorphosed altered volcanic rocks around the Snow Lake VMS deposits contain mineral assemblages that include garnet, staurolite, kyanite, quartz, chlorite, biotite, muscovite, and quartz (Hutcheon 1979, Froese & Moore 1980, Zaleski *et al.* 1991). Metasedimentary rocks at similar metamorphic grade from the town of Snow Lake are staurolite-bearing metaturbidites (Kraus & Williams 1994). We found samples containing the assemblage garnet + chlorite + quartz to be useful for textural analysis because they clearly display the relation between garnet growth and deformational events. Garnet grains in these samples overgrew the chlorite + quartz matrix, successively incorporating quartz grains and preserving the sequence of deformational microfabrics. We also examined samples from a number of different alteration zones that at garnet grade contained the assemblage garnet + biotite + chlorite + plagioclase + quartz + muscovite ± staurolite, in order to obtain detailed correlation of structural events with metamorphic events across the region. These samples were used for analysis of P–T path because they have a relatively low variance and contain minerals that preserve compositional zoning.

TABLE 1. MINERAL ASSEMBLAGES CONTAINING MUSCOVITE, PHOTO LAKE DEPOSIT

Ky + Bt + Chl +	Qtz + Ms
Ky +	Qtz + Ms
St + Grt + Bt + Pl +	Qtz + Ms + Mag
St + Grt + Bt +	Qtz + Ms + sulfides
St + Bt + Chl + Pl +	Qtz + Ms + sulfides
St + Bt + Pl +	Qtz + Ms + sulfides
St + Bt +	Qtz + Ms + sulfides
St + Pl +	Qtz + Ms + sulfides
Grt + Bt + Pl +	Qtz + Ms + Opq
Bt + Pl +	Qtz + Ms + sulfides
Bt + Chl +	Qtz + Ms + Ilm
Bt + Ep +	Qtz + Ms
Bt +	Qtz + Ms + Opq
Chl +	Qtz + Ms

Opq = Ilm, Mag, or sulfides

A key element of the metamorphic P–T paths described below is the interpretation of the mineral assemblage present at the time of garnet growth. A significant challenge in the interpretation arises where some minerals previously in the garnet-grade assemblage are not preserved in the final assemblage. Chlorite, for example, is commonly consumed during growth, and there may or may not be any chlorite left over at the end of garnet growth. In our opinion, the chlorite was consumed during garnet growth in all samples described here, on the basis of phase petrology, correlation from rocks where it is still present, and our experience in other terranes, where the abundance of chlorite decreases with increasing grade and growth of garnet (Menard & Spear 1994).

In our opinion also, some samples described below contained muscovite during garnet growth. Muscovite is common in altered volcanic rocks from Snow Lake, and the mineral assemblages of samples that still contain muscovite are listed in Table 1. These assemblages are similar to those in metapelites; thus it is not surprising that muscovite may have been present during growth of garnet in some rocks. Sample CH93–11–3601, described below, contains no muscovite or plagioclase, and only minor biotite, and likely never contained significant amounts of muscovite. The other samples described, in contrast, do contain biotite and plagioclase. They likely also contained muscovite, by analogy with samples from the area that still do contain muscovite, but the muscovite was consumed during prograde metamorphism.

We contend that some samples described below contained epidote or calcite during garnet growth. An additional Ca-bearing phase such as epidote or calcite is required if there was simultaneous net growth of garnet and plagioclase. Epidote and calcite are commonly consumed in calcic pelites during growth of garnet and plagioclase, and it can be difficult to find traces of them

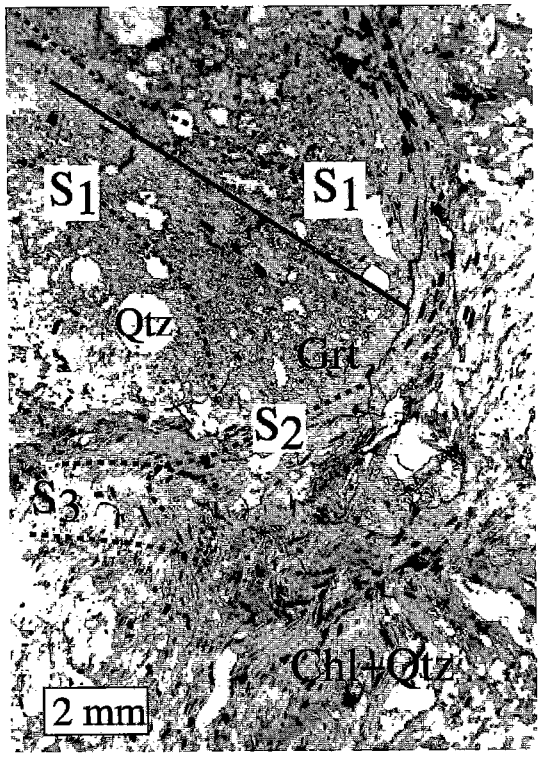

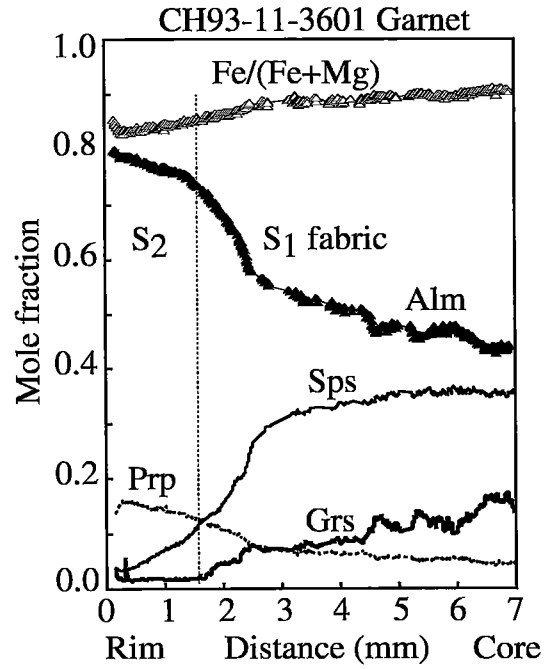

FIG. 3. Deformational fabrics at Snow Lake. (a) Photomicrograph of sample CH93–11–3601 showing three deformational fabrics: the garnet core overgrew the S_1 fabric early during F_2, the rim overgrew the S_2 fabric, and the S_2 fabric in the matrix was crenulated by F_3. (b) Compositional zoning of garnet in sample CH93–11–3601 along traverse indicated in (a). Note that Fe/(Fe + Mg) decreases continuously across the textural break (dashed line) marked by the trails of inclusions. The symbols mark locations of 633 analyses.

TABLE 2. MINERAL COMPOSITIONS USED FOR REPRESENTATIVE P–T RESULTS

Sample	Mineral	#	SiO_2	Al_2O_3	TiO_2	MgO	FeO	MnO	CaO	Na_2O	K_2O	ZnO	Wt% Total
DUB54-1401	Grt A rim	3	37.7	21.1	na	3.90	30.4	5.81	2.60	na	na	na	101.5
DUB54-1401	Grt A core	3	37.6	20.8	na	2.68	26.2	9.73	3.73	na	na	na	100.7
DUB54-1401	Grt B core	3	37.5	19.6	na	1.65	21.1	15.40	4.71	na	na	na	100.0
DUB54-1401	Bt	3	37.0	18.9	na	13.80	16.6	<0.20	0.50	<0.20	9.17	na	96.0
DUB54-1401	Chl retro	3	25.6	23.9	<0.20	20.50	19.9	0.24	<0.20	<0.20	<0.20	na	90.1
DUB85-1137	Chl	8	25.0	24.1	0.06	16.10	24.2	0.06	<0.20	<0.20	<0.20	na	89.5
DUB85-1137	Grt rim	3	37.8	22.2	na	2.89	34.7	1.30	2.48	na	na	na	101.4
DUB85-1137	Grt core	3	37.7	22.1	na	1.44	29.1	7.30	4.01	na	na	na	101.7
ZYL124-552	Grt rimmost	3	37.7	21.3	na	3.65	33.2	3.58	2.24	na	na	na	101.7
ZYL124-552	Grt near rim	3	38.6	21.6	na	7.64	29.8	1.07	2.41	na	na	na	101.1
ZYL124-552	Grt plateau	3	38.6	22.0	na	7.25	30.0	1.23	2.79	na	na	na	101.9
ZYL124-552	Ged	4	42.9	17.4	0.25	13.00	23.2	0.40	0.51	1.63	<0.20	na	99.3
ZYL124-552	St in Grt	14	26.9	54.9	0.59	3.54	12.7	0.12	<0.20	<0.20	<0.20	1.29	100.1
ZYL124-552	Bt	9	37.6	18.1	1.30	14.00	15.9	<0.20	<0.20	0.60	8.31	na	95.8

#: number of analytical data-sets averaged; retro: retrograde phase; in Grt: included in garnet; na: not analyzed.

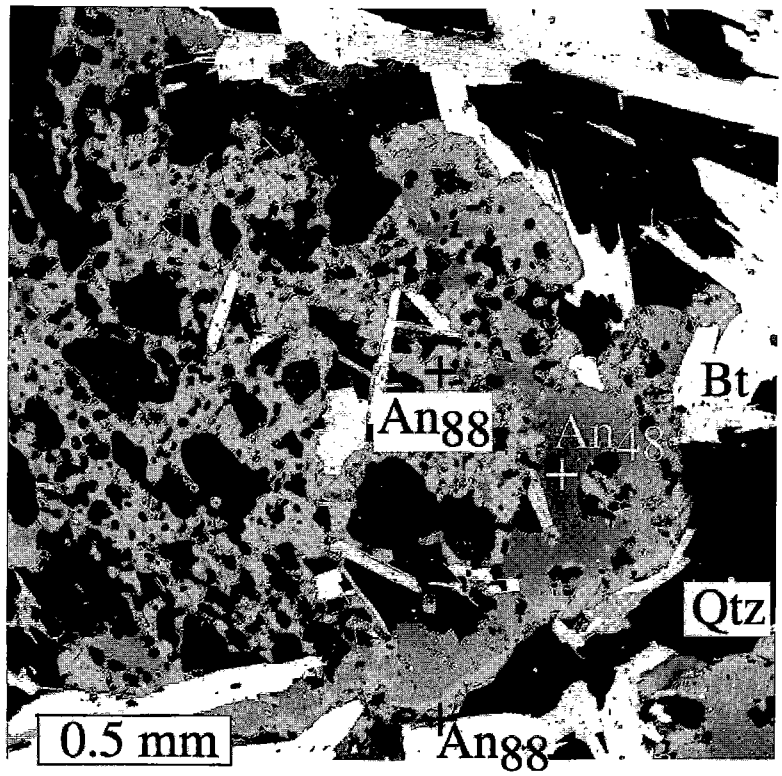

FIG. 4. Back-scattered electron image of plagioclase in sample DUB54–1401, showing a calcic core with abundant inclusions of quartz and a compositionally zoned rim with fewer inclusions.

in the rock (unpubl. data). Their early presence in a rock can be interpreted from phase petrology (simultaneous growth of garnet and plagioclase), rare inclusions in porphyroblasts, correlation from other similar rocks that still contain epidote or calcite, and the development of garnet with elevated and fairly constant proportion of the grossular component, X_{Grs} (Menard & Spear 1993).

Thus, we contend that some samples had an assemblage during garnet growth that is characteristic of metasedimentary calcic pelitic schists. Menard & Spear (1993) described the phase petrology of calcic pelitic schists from Vermont. One of their samples, TM825A from the Elizabeth Cu deposit, is a coarse garnet schist that is strikingly similar to samples DUB54–1401 and DUB85–1137 (described below). These three rocks contain large (1–4 cm) porphyroblasts of garnet, with trails of inclusions that preserve an early schistosity and contain plagioclase zoned with X_{An} increasing toward the rim. Sample TM825A is also very similar to associated samples of calcic pelitic schist in Vermont in terms of the suite of minerals included in porphyroblasts, the textures of inclusion trails in porphyroblasts, the compositions of minerals, the patterns of compositional zoning of minerals, the calculated pressure and temperature, and the calculated P–T path (Menard & Spear 1993). The main differences are that sample TM825A contains larger crystals of garnet, less muscovite, and more plagioclase, which made the coarse garnet schist a mappable unit. Slack (1997a, b) re-interpreted the coarse garnet schists in Vermont as altered mid-ocean-ridge basalts on the basis of trace-element geochemistry. Thus, the altered volcanic rocks and the metasedimentary calcic pelitic schists in Vermont have similar mineral assemblages and similar metamorphic histories. A similar origin as altered volcanic rocks is obvious for the coarse garnet schists from Snow Lake, suggesting that the coarseness of the garnet from Snow Lake and from Vermont may be related to minor peculiarities in the bulk-rock composition of metamorphosed altered volcanic rocks.

A description of our samples and data follows.

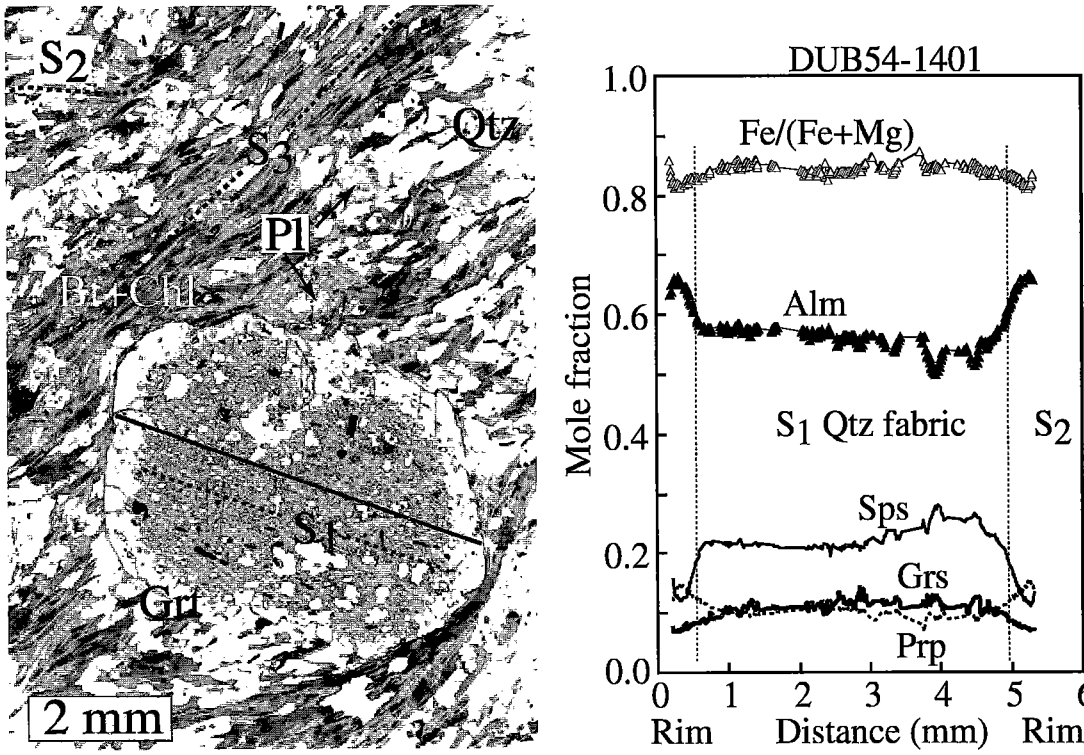

FIG. 5. Simple garnet in sample DUB54–1401. (a) Photomicrograph showing S_1 fabric in the garnet core, and S_2 and S_3 fabrics in the matrix. The dark mica is biotite, the pale phyllosilicate is chlorite, and quartz and plagioclase appear white. (b) Compositional traverse across garnet in (a) (178 data points).

MICROSTRUCTURES AT SNOW LAKE

We recognize three distinct deformational fabrics in samples of altered metavolcanic rocks from Snow Lake. S_1 and S_2 schistosities developed during prograde metamorphism at chlorite grade and near the thermal peak, respectively. They were both well developed, but S_2 commonly obscures S_1. Consequently, S_1 is best preserved as trails of inclusions within porphyroblasts. S_3 crenulation of S_2 developed during retrograde metamorphism at chlorite grade.

All three fabrics are exhibited in sample CH93–11–3601 (Fig. 3a), from near Chisel Lake (UTM 14U 6077800mN, 428900mE). The sample contains the assemblage garnet + chlorite + quartz + ilmenite, with minor biotite, sulfides, apatite, monazite, and zircon. It has less than 0.02% (by weight) K_2O and Na_2O, and consequently contains no plagioclase or muscovite, and only minor biotite. Chlorite, quartz, and ilmenite in the matrix display an S_2 schistosity that was subsequently crenulated by F_3 (Fig. 3).

In this sample, S_1 and S_2 are displayed as internal foliations in garnet porphyroblasts, which typically have a pink core with abundant inclusions (quartz, ilmenite, chlorite, apatite, monazite, and trace sulfides) and a purple rim with few inclusions (Fig. 3). Abundant inclusions of quartz in the core display a weak, slightly bent S_1 fabric. Some round aggregates of quartz grains 1–2 mm across in the garnet core may be relict, recrystallized volcanic phenocrysts (Fig. 3a). The garnet rim contains inclusions of ilmenite aligned continuously with the matrix S_2 fabric, but at a high angle to trails of inclusions in the core. Garnet growth occurred during F_2, as indicated by bending of S_1 trails in the garnet core, and continued until after S_2 was fully developed, as indicated by the rim that overgrew S_2. Furthermore, garnet growth predated F_3, as indicated by the F_3 crenulation cleavage, which is found only in the matrix and not inside the garnet.

Fe/(Fe + Mg) zoning of the garnet decreases continuously from core to rim (Fig. 3b), which may indicate increasing temperature during garnet growth in this assemblage, by analogy with pelitic assemblages (Spear *et al.* 1990). The continuity of compositions from core to rim suggests that growth of garnet occurred throughout development of the S_2 fabric.

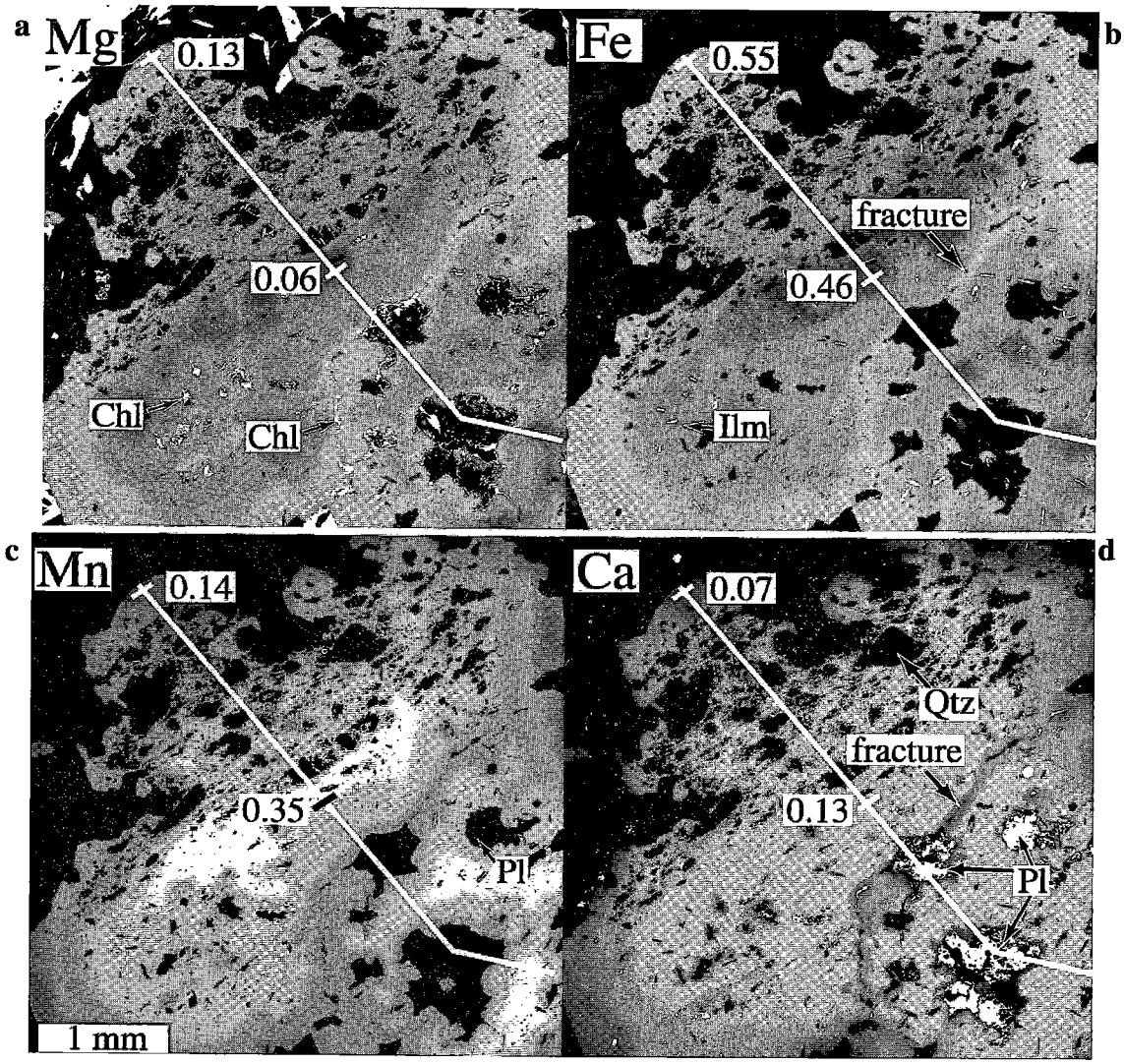

FIG. 6. Complex garnet in sample DUB54–1401. (a, b, c, d) X-ray compositional maps of garnet zoning. The Ca zoning pattern suggests that the garnet core was fractured and healed by continued growth of garnet with lower X_{Grs}.

P–T PATH AT SNOW LAKE: SAMPLE DUB54–1401

Description

Sample DUB54–1401 from the Photo Lake deposit (UTM 14U 6080000mN, 429300mE) is an altered volcanic rock, for which a metamorphic P–T path was computed. The sample contains the assemblage garnet + biotite + plagioclase + quartz + ilmenite + pyrrhotite + chalcopyrite + sphalerite + S_3 chlorite, with minor staurolite, zincian spinel, apatite, and trace retrograde pyrite. Most of the sulfide is concentrated in a single layer in the sample, and appears not to have participated in net-transfer reactions with the silicate minerals. Biotite and chlorite are oriented in S_2, which is a crenulation fabric of S_1. Minor variation of biotite compositions (Al ranges from 1.63 to 1.73 atoms per formula unit, *apfu*, for example) may reflect partial modification during F_3 (Table 2). Compositions of chlorite are fairly uniform in the sample, with Fe/(Fe + Mg) ranging from 0.345 to 0.358.

Plagioclase grains in this sample are zoned, with a core of composition An_{88} separated by a sharp break from a rim in which X_{An} increases outward from An_{48} to An_{88} (Fig. 4). The core of plagioclase grains contains abundant inclusions of quartz, whereas the rim contains

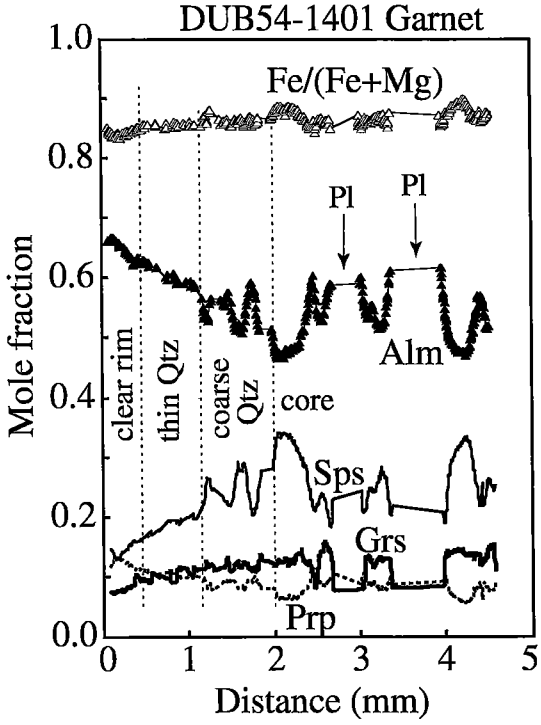

Fig. 6.e. Compositional zoning along traverse shown in X-ray maps. Arrows point to locations of plagioclase inclusions. The inclusion-free garnet rim and the zone of coarse inclusions of quartz correlate with the rim and core of the garnet in Figure 5. Smoothly curved zoning of Fe, Mg, and Mn around plagioclase inclusions and the fracture suggest a late episode of compositional modification by diffusion, in contrast with the step-function change in X_{Grs} (550 data points).

few inclusions. Fine laminations in the compositional zoning of some plagioclase grains replaced the S_2 foliation, which indicates that they postdate the S_2 foliation (not shown). Compositions of the rim of plagioclase grains in the matrix are similar to those of plagioclase included in the garnet. Some plagioclase grains were partially replaced by a second generation of biotite and chlorite, which likely are F_3 minerals.

In some grains of garnet, the core (X_{Alm} = 0.58) contains abundant inclusions of quartz that display a faint shape fabric, whereas the rim (X_{Alm} = 0.65) contains few inclusions (Fig. 5). The core of these grains overgrew the S_1 fabric, and the rim overgrew the S_2 fabric, as in sample CH93–11–3601 (above). Plagioclase grains with compositions of An_{85-80} partially replaced the rim, and hence postdate the growth of the garnet.

The complete history of garnet compositions, however, is more complicated. A second type of grain of garnet (Fig. 6) has a rim with few inclusions and the same compositions as the previously described grain, a zone near the rim of thin inclusions of quartz that displays the S_2 fabric, an inner zone of coarse inclusions of quartz with some compositions matching the post-S_1 core of the first, and patches in the core with few inclusions and higher X_{Sps} than the above-described garnet. These zones of high X_{Sps} in the core likely are older than the garnet in Figure 5. X_{Grs} in the core exhibits a sharp break in composition along an irregular zone that could have been a fracture healed by later growth of garnet. The other components, in contrast, are smoothly zoned in this region, possibly the result of minor, late modification by diffusion superimposed on a step-function zoning patterns similar to X_{Grs}.

Reaction history

Matrix plagioclase (Fig. 4) and the first garnet grain (Fig. 5a) both display similar textures of trails of inclusions and hence likely grew at the same time. Thus, the decrease of X_{An} from An_{88} to An_{48} occurred during development of the S_2 fabric, and correlates with the core–rim break in the first garnet. The correlation of the increase X_{An} in the plagioclase rim to the garnet is less certain, as the plagioclase may have grown after garnet growth ceased. The simplest interpretation is that X_{An} decreased during growth of the garnet, and increased during subsequent consumption of garnet. Garnet may have grown by a reaction like: Chl + Ms + Qtz = Grt + Bt + Pl + H_2O. During F_3, minor chlorite grew at the expense of plagioclase and biotite.

Thermobarometry

Using the garnet composition with the lowest X_{Sps} near the rim of the grains and matrix biotite or chlorite compositions gives temperatures of approximately 560°C and 530°C, respectively. Using the garnet, biotite, An_{48} plagioclase, with a fictitious pure muscovite gives maximum pressures of 3.5–5.0 kbar (assuming 550°C). The range of pressures results from differences in the calibrations used. Using the same minerals without muscovite gives pressures of 4.1 to 4.2 kbar (assuming 550°C). Use of WebINVEQ with garnet + biotite + plagioclase + muscovite gives similar results, 570°C and 4.8 kbar.

P–T path

Figure 7 shows the P–T path constructed for the time of garnet growth in this sample in the assemblage garnet + biotite + chlorite + plagioclase + quartz + muscovite + H_2O (Table 3). The problem has a phase-rule variance of four, and a two-point path was calculated using X_{Alm}, X_{Sps}, X_{Grs}, and X_{An} as monitor variables. The P–T path for the time of garnet growth was computed backward in time from rim to core, but paths are

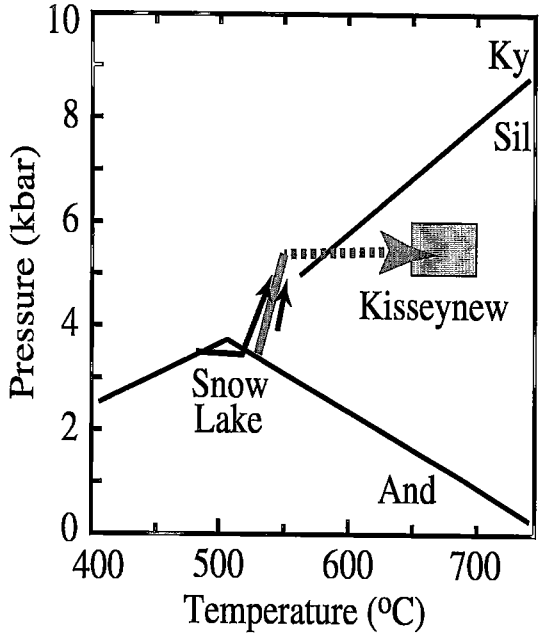

FIG. 7. Metamorphic P–T paths for F_2 deformation determined in this study (solid arrows). Black arrows calculated for samples from the Photo Lake mine in Snow Lake; shaded arrow is estimated for samples from Wolverton Lake in the Kisseynew Domain (see Fig. 15). Both locations experienced increasing pressure during F_2 deformation at approximately the same time and P–T conditions, but subsequent heating was much greater in the Kisseynew Domain than at Snow Lake (dashed portion of grey arrow). The shaded box outlines the range of thermobarometric estimates of the peak conditions of metamorphism for the Kisseynew samples.

TABLE 3. STARTING CONDITIONS FOR THE MODELS

DUB54-1401
SiO_2–Al_2O_3–MgO–FeO–MnO–CaO–Na_2O–K_2O–H_2O
DUB85-1137
SiO_2–Al_2O_3–MgO–FeO–MnO–CaO–Na_2O–H_2O
ZYL134-552
SiO_2–Al_2O_3–MgO–FeO–MnO–ZnO–CaO–Na_2O–K_2O–H_2O

	DUB54-1401	DUB85-1137	ZYL134-552
P (kbar)	5.0	5.0	5.5
T (°C)	550	540	550
garnet	yes	yes	15%
X_{Prp}	0.149	0.116	0.284
X_{Alm}	0.654	0.783	0.617
X_{Sps}	0.126	0.031	0.023
X_{Grs}	0.071	0.072	0.076
staurolite	no	no	13%
X_{Mg}			0.32
X_{Fe}			0.64
X_{Zn}			0.08
chlorite	yes	yes	15%
X_{Mg}	0.646	0.700	0.747
X_{Fe}	0.35	0.298	0.250
X_{Mn}	0.004	0.002	0.003
biotite	yes	no	10%
X_{Mg}	0.595		0.688
X_{Fe}	0.4		0.310
X_{Mn}	0.005		0.002
plagioclase	yes	yes	5%
	An_{48}	An_{45}	An_{58}
muscovite	yes	no	14%
quartz	yes	yes	25%
H_2O	yes	yes	3%

consistently reported in the forward direction. During growth of garnet, which textures show overlapped F_2, pressure increased by 1.1 kbar and temperature by 12°C. Uncertainty in this path may be as much as 10–25% of the changes in pressure and temperature, as a result of counting statistics in the analytical data, real compositional variability, and uncertainties in the thermodynamic data and mixing models. However, that does not affect the shape of the path or the tectonic implications. The critical factor for uncertainty in the path is the correlation of mineral compositions.

P–T PATH AT SNOW LAKE: SAMPLE DUB85–1137

Description

Sample DUB85–1137 (Fig. 8) is also from the Photo Lake deposit (UTM 14U 6080000mN, 429300mE). It contains the assemblage garnet + chlorite + plagioclase + quartz + magnetite, with minor pyrite, ilmenite and calcite. Garnet porphyroblasts contain inclusions of quartz that display a shape fabric in the garnet core and middle region (Fig. 9). The size of the quartz inclusions decreases from the core (20 × 60 μm and 20 × 100 μm) to the middle region (5 × 20 μm and 2 × 5 μm), although some larger grains relict from the time of growth of the garnet core also are included in the middle region. Quartz grains included in the core and middle region were resorbed by continued growth of garnet, as shown by facets on the garnet crystal impinging into the inclusions, obscuring the original ellipsoidal shapes of the inclusions. The garnet rim, by contrast, contains coarser (15 × 30 μm), unoriented inclusions of quartz. Thus the garnet core overgrew an S_1 fabric with thin grains of quartz, the garnet middle region overgrew a later fabric with thinner grains of quartz, and the rim overgrew the S_2 fabric with relatively coarse grains of quartz. In other samples, a similar coarsening of quartz grains is associated with the development of the S_2 schistosity. Apparently, S_1 was subparallel to S_2 at this location, or was rotated into parallelism. The absence of sharp textural breaks suggests that the garnet grew during a single metamorphic event that spanned F_2 deformation.

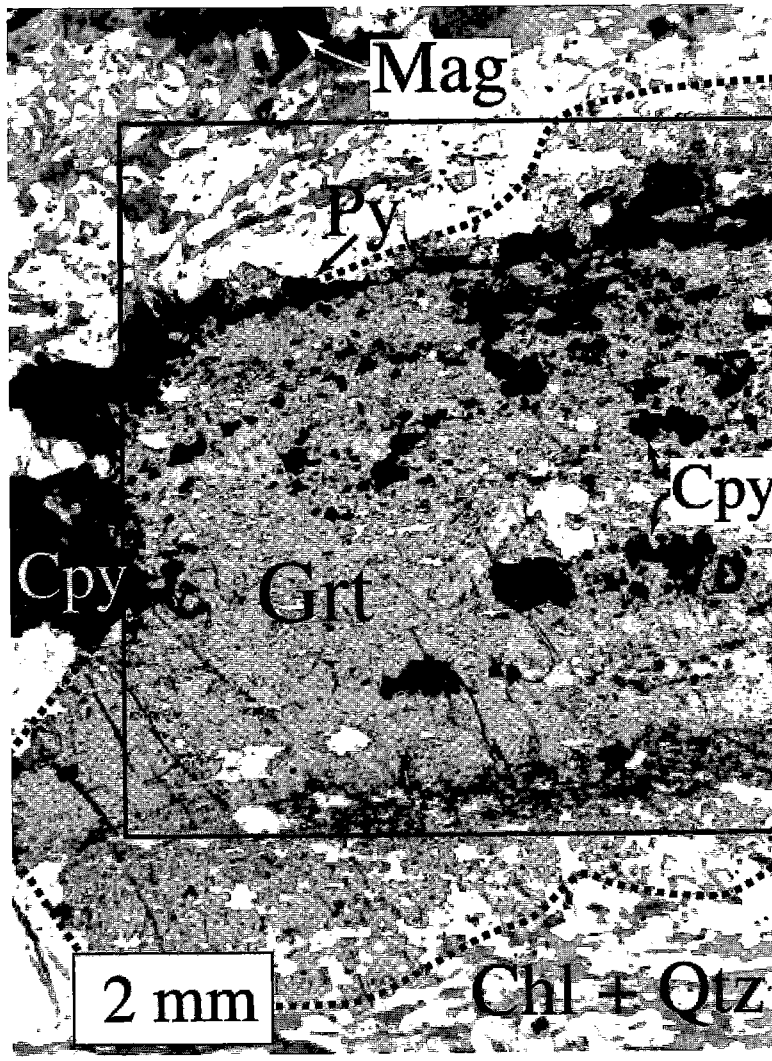

FIG. 8. Photomicrograph of sample DUB85–1137 showing garnet and S_1/S_2 fabric in matrix.

Garnet also contains inclusions of chalcopyrite, pyrite, and minor sphalerite in the core and middle region, and inclusions of magnetite in the rim (Fig. 9), indicating a change of assemblage from core to rim. The sulfide inclusions are resorbed and partially replaced by garnet, further indicating consumption of sulfides during growth of garnet. In addition, garnet contains inclusions of ilmenite, the core contains inclusions of calcite, and the middle region contains abundant inclusions of chlorite and minor An_{36} plagioclase.

Garnet is compositionally zoned in domains (Fig. 9). Around inclusions of sulfide, values of X_{Alm} and X_{Sps} are similar to those at the rim. In contrast, X_{Grs} is uniformly higher in the core than in the rim. These features suggest that X_{Alm} and X_{Sps} around sulfide inclusions were modified by diffusion after garnet growth. In a similar manner, compositions of the middle region of the garnet around the abundant inclusions of chlorite may have been modified by localized re-equilibration by diffusion.

The cores of plagioclase grains overgrew a thin quartz shape fabric (4 × 20 μm, with some 20 × 100 μm), whereas their rims contain few inclusions of quartz grains (Fig. 10). Plagioclase grains are compositionally zoned from An_{44} in the core to

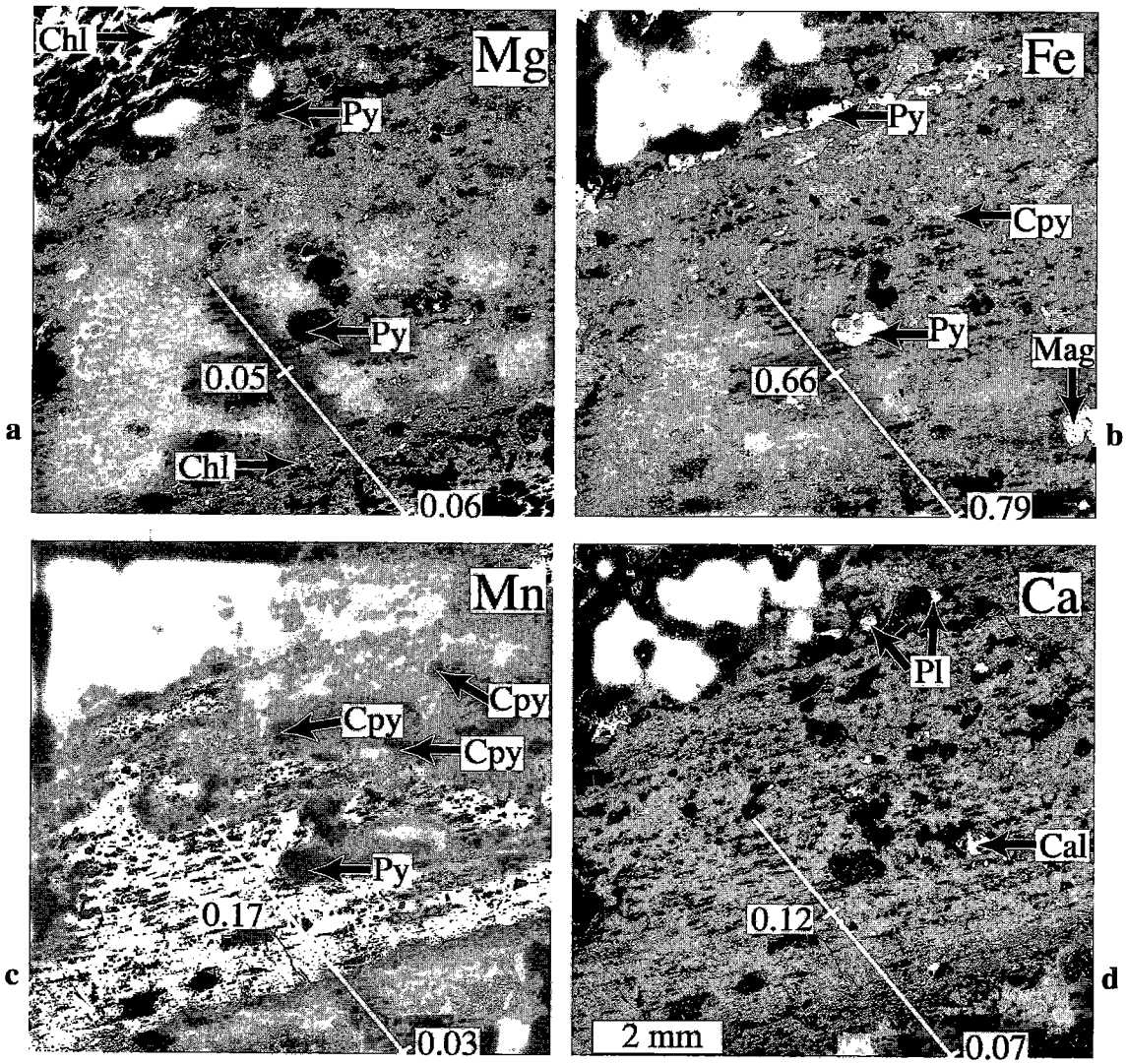

FIG. 9. Garnet in sample DUB85–1137. (a, b, c, d) X-ray compositional maps of garnet zoning.

An_{68} just beyond the thin quartz inclusions to An_{43} at their rim. Trails of inclusions in the core of plagioclase grains vary in orientation from grain to grain, reflecting rotation of grains with respect to each other during F_3 crenulation.

Chlorite occurs as coarse, undeformed (recrystallized) grains aligned in the S_1–S_2 fabric and in the S_3 crenulation fabric (Fig. 9). Coarse grains of quartz are interpreted as being formed during S_3.

Reaction history

The petrography suggests that garnet and plagioclase grew by a reaction like:

$$Chl + Cal + Qtz = Grt + Pl + fluid$$

Calcite is preserved as relict inclusions in garnet. Furthermore, the petrography suggests that sulfides were removed from the sample during F_2 and associated growth of garnet by a reaction like:

$$Cpy + Py + Sp + O_2 = Mag + Cu^{2+} + Zn^{2+} + S^{2-}$$

Correlation of plagioclase compositions with garnet compositions is shown in Figure 9e. The rims of plagioclase and garnet are correlated on the basis of the sparseness of inclusions compaired to their cores. The core and the An_{68} ring in plagioclase contain the same size of quartz inclusions as does the middle region of

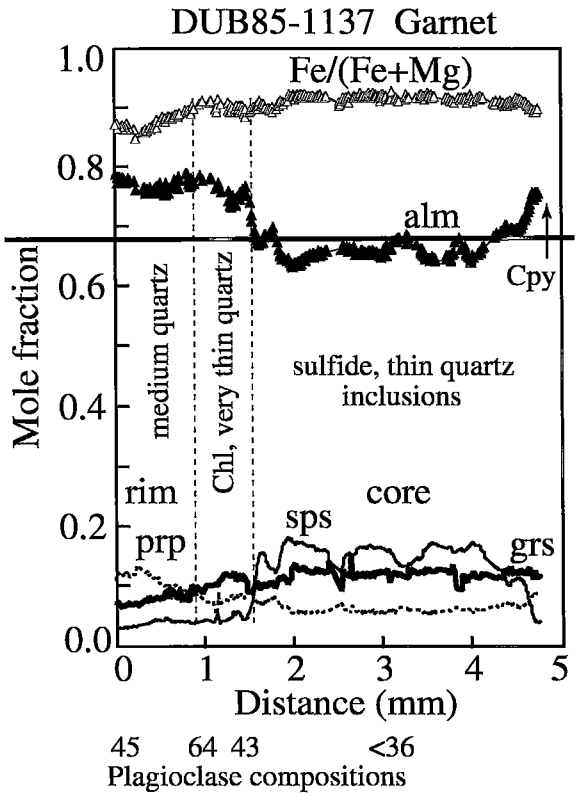

Fig. 9.e. Compositional traverse across garnet shown in Figure 8 and 9a, b, c, and d. Garnet compositions were modified around sulfide inclusions in the garnet core (322 data points). Also shown are An contents of correlated plagioclase

the garnet, indicating that these zones correlate. Inclusions of An_{36} plagioclase in the middle region and outer portion of the garnet core support this correlation, and suggest that the garnet core grew with lower X_{An} (possibly An_{28-30}) plagioclase. The sequence of quartz textures during metamorphism is preserved in garnet grains in this and other samples, and suggests that correlation on the basis of these textures is reliable even though quartz was a reactant during garnet growth.

Thermobarometry

Thermometry using matrix chlorite with the lowest Fe/(Fe + Mg) garnet near the rim gives a temperature of *ca.* 540°C (assuming 5 kbar). In the absence of good barometers applicable to the assemblage in this sample, metamorphic pressures for the garnet rim were assigned as 5.0 kbar, consistent with data from other samples (above and unpubl. data), from Zaleski *et al.* (1991), and from Kraus & Menard (1997).

P–T path

A P–T path (Fig. 7) was computed for the time of garnet growth in this sample in the assemblage garnet + chlorite + plagioclase + clinozoisite + quartz + H_2O (Table 3). Clinozoisite is used as an approximation for calcite observed as inclusions in the garnet in order to reduce the variance of the problem to 4. Calculations in other assemblages indicate that this approximation produces only minor changes in the phase petrology computed (unpubl. data). Furthermore, clinozoisite may have been in the assemblage, even though relics were not found. The correlations of plagioclase with garnet discussed above were used in computing the path for the time spanning the development of the S_2 foliation. This path shows a temperature increase of 30–40°C, followed by heating of 25°C and a pressure increase of 1.3 kbar.

Metamorphism in the Southern Kisseynew Domain

Samples from the south flank of the Kisseynew Domain (Fig. 1) were collected from an alteration zone around a VMS deposit at the south end of Wolverton Lake, 8 km northeast of Snow Lake. Additional samples collected from the Wim VMS deposit on the west side of the Herblet Lake gneiss dome (Fedikow & Ziprick 1991) 16 km northeast of Snow Lake display a similar metamorphic history, but are not described here. Gneisses from the central Kisseynew Domain contain the assemblages sillimanite + garnet + biotite or garnet + cordierite, indicating that the peak pressure was less than 6 kbar (Bailes & McRitchie 1978, Spear 1993).

Microstructures in the Southern Kisseynew Domain

Sample ZYL134–513, from the south end of Wolverton Lake (UTM 14U 6090800mN, 440200mE), contains the assemblage sillimanite + staurolite + garnet + biotite + quartz, with minor ilmenite, monazite, pyrite, and chalcopyrite. The core of garnet grains contains inclusions of fine-grained quartz that display an S_1 shape fabric (Fig. 11). The rim of the garnet grains, in contrast, contains few inclusions of medium-grained quartz. The same textures occur in samples from Snow Lake (see above), suggesting comparable and possibly correlative growth of garnet and development of an S_2 fabric in both places. The assemblage at the time of garnet growth (garnet + biotite + chlorite + quartz + ilmenite) suggests temperatures of 500–550°C, on the basis of our experience with similar rocks from other locations. Thermobarometric calculations for the time of F_2 development were not made for this sample because of the lack of plagioclase.

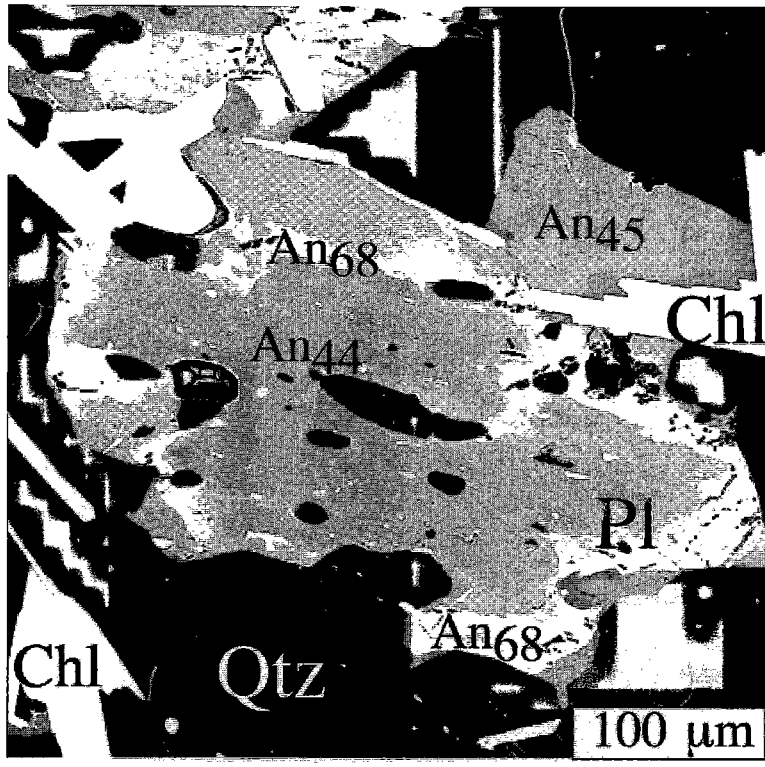

FIG. 10. Back-scattered electron image of plagioclase in sample DUB85–1137. The size and shape of the quartz inclusions suggest that the core and rim correlate with the middle region and rim of the garnet, respectively.

P–T PATH IN THE KISSEYNEW DOMAIN: SAMPLE ZYL134–552

Description

Sample ZYL134–552 is from the same drill hole as sample ZYL134–513 (above). It is a gneiss that contains the assemblage garnet + biotite + plagioclase + gedrite + quartz + retrograde chlorite (Fig. 12). The gedrite contains inclusions of quartz, ilmenite, plagioclase, and biotite. Porphyroblasts of gedrite are generally oriented in the gneissic foliation, and hence grew later than garnet (see below). Minor retrograde chlorite partially replaced garnet and biotite.

Inclusions in the garnet core are relatively small and euhedral (Fig. 12), inclusions in a middle region are coarser, and inclusions in the garnet rim are sparse. Other samples from the same drill hole indicate that this textural change from the middle region to the rim marks the development of a deformational fabric older than the gneissosity. By correlation with the previous sample, we interpret the garnet-grade foliation as S_2.

Compositional zoning of garnet is shown in Figure 13. The garnet exhibits a general trend of decreasing X_{Sps} from core to rim, and slightly increasing X_{Grs} up to a plateau near the rim. Fe/(Fe + Mg) increases sharply in the outermost 1 mm of the garnet, in a pattern following the resorbed edges of the garnet, indicating that it is a relatively late, retrograde modification (later than possible re-equilibration by diffusion at peak conditions).

Porphyroblasts of garnet contain inclusions of staurolite, plagioclase, biotite, chlorite, quartz, and ilmenite. Compositions of plagioclase inclusions in garnet are strikingly zoned with respect to position in the grains of garnet (Fig. 14). Some plagioclase grains in the center of the garnet core have compositions of An_{91}, whereas others are zoned from An_{67} to An_{87}, indicating increase of X_{An} prior to growth of garnet. In the middle region, compositions of the rim of plagioclase inclusions decrease to An_{54} with increasing distance from the core of the garnet. Near its rim, one plagioclase inclusion is zoned from An_{44} to An_{58}, indicating a late increase of X_{An} during garnet growth.

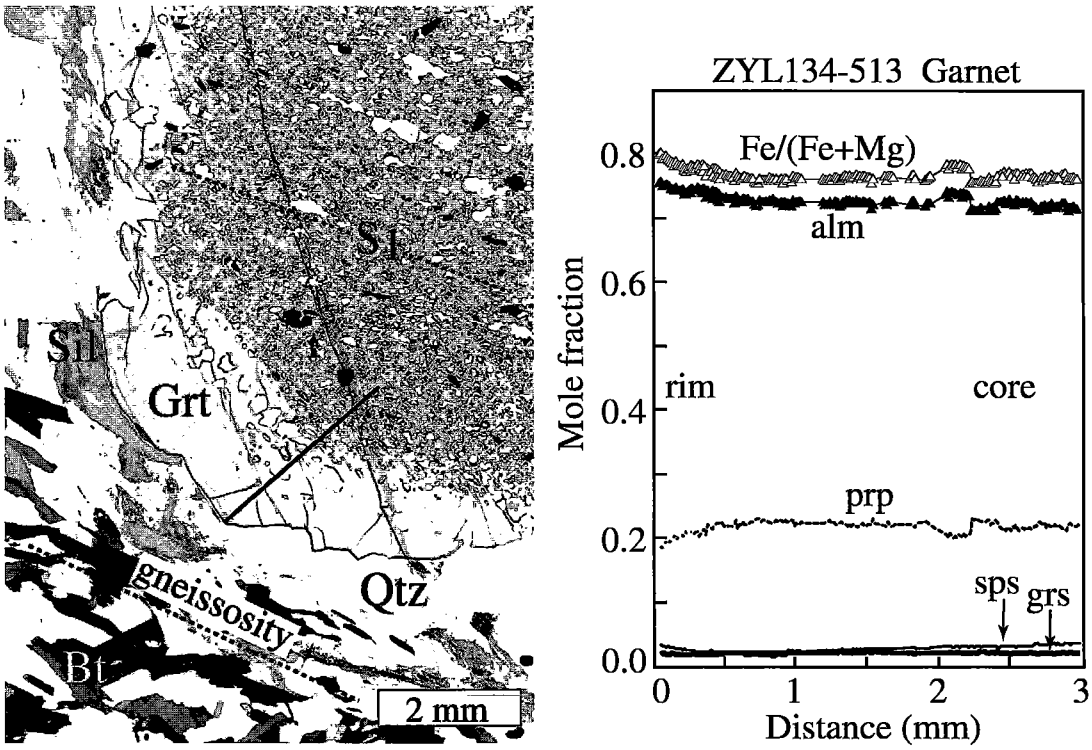

FIG. 11. F_2 garnet in a Kisseynew gneiss. (a) Photomicrograph of sample ZYL134–513 showing relation between garnet and the foliation. The garnet core contains trails of inclusions of quartz, but the rim contains fewer inclusions, as in Figure 3, suggesting a similar relation between F_2 deformation and metamorphism. (b) Compositional zoning along traverse shown in (a). The relatively flat zoning suggests homogenization at high grade, with possible modification during cooling to raise X_{Alm} and Fe/(Fe + Mg) at the rim.

Staurolite occurs only as inclusions in garnet and plagioclase. Staurolite grains included in the garnet core are euhedral, whereas those in the middle region of the garnet were partially resorbed, indicating partial consumption of staurolite during growth of garnet. Furthermore, staurolite compositions vary with position in the garnet, from 0.18 atoms Zn per 48 atoms of oxygen in the garnet core to 0.39 atoms Zn in the garnet rim. Relict grains of staurolite included in plagioclase, by comparison, contain up to 0.47 *apfu* Zn, reflecting continued consumption of staurolite. Although the compositions appear stoichiometric (Table 2), the sum of the octahedrally coordinated cations is near 5, which suggests that the grains may be a rare occurrence of anhydrous staurolite (*cf.*, Hawthorne *et al.* 1993, Holdaway *et al.* 1995). The Fe/(Fe + Mg) of staurolite inclusions varies with the composition of the surrounding garnet, allowing the interpretation that Fe and Mg of the staurolite were modified during diffusion of cations in the garnet. The same high-temperature event may have dehydrated staurolite grains preserved as isolated relics in the garnet, whereas staurolite grains in the matrix reacted with quartz and were removed.

In the matrix, plagioclase grains are compositionally zoned from An_{91} to An_{53} where they progressively replaced relict staurolite. Thus, replacement of staurolite by plagioclase correlates with plagioclase inclusions in the middle region of the garnet. Other plagioclase grains are zoned from An_{53} to An_{56}, which suggests that they grew at the same time as those in the garnet rim.

Reaction history

Prior to growth of garnet, the sample was fine grained and contained the assemblage chlorite + biotite + muscovite + plagioclase (An_{91}) + calcite + quartz + ilmenite. The presence of muscovite is suggested by subsequent growth of biotite and correlation with muscovite-bearing samples from VMS deposits at lower metamorphic grade. Growth of plagioclase with increasing X_{An} prior to garnet growth suggests that a Ca-bearing phase such as calcite was present early.

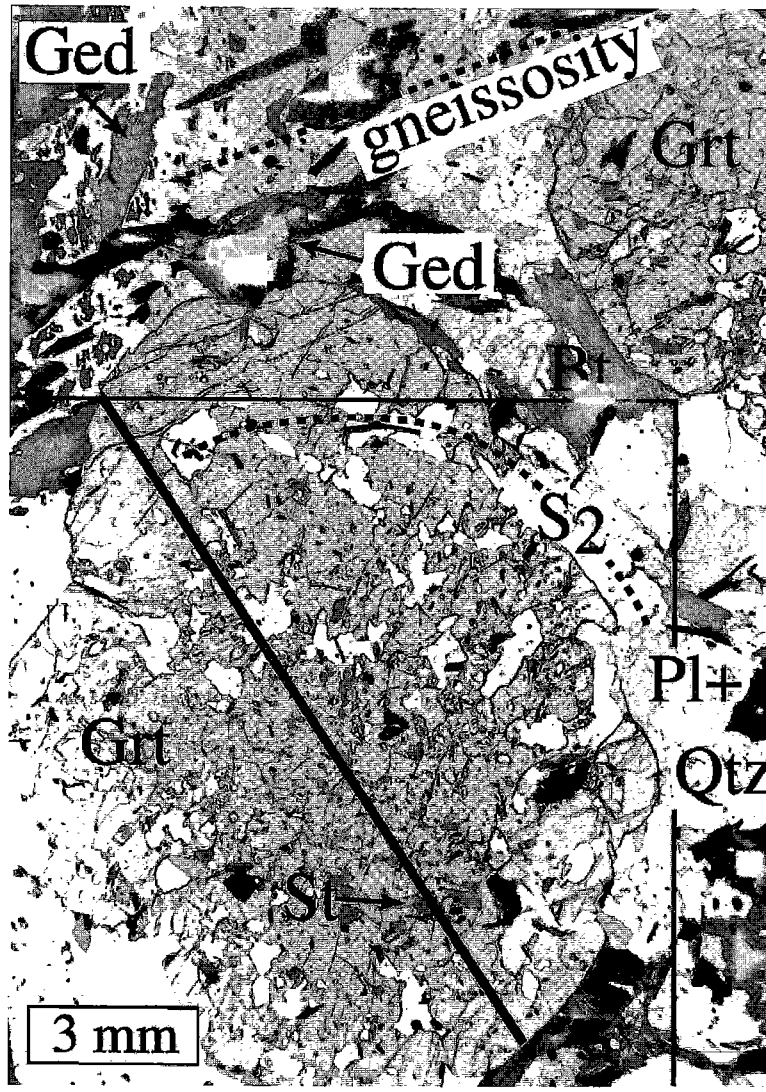

FIG. 12. Photomicrograph of sample ZYL134–552 showing garnet that grew during F_2, inclusions of plagioclase and staurolite in the garnet, and gedrite aligned in gneissic fabric. The location of Figure 14 is outlined.

Subsequent consumption of plagioclase and growth of the garnet core and middle region occurred by a reaction such as: chlorite + plagioclase + muscovite + staurolite + quartz = garnet + biotite + fluid. When the rim plateau grew, staurolite was effectively gone from the assemblage, and X_{An} started to increase. Subsequently, temperature increased, the gneissosity was developed, gedrite, some biotite, and some plagioclase grew, and quartz recrystallized and coarsened.

Thermobarometry

Thermometry based on compositions of the garnet rim and biotite in contact with garnet yields temperatures near 530°C, which are much lower than the peak temperature (see below). This finding supports the interpretation above that the garnet rim was modified during cooling. The effects of retrograde modification of composition appear to be limited to the edge of the

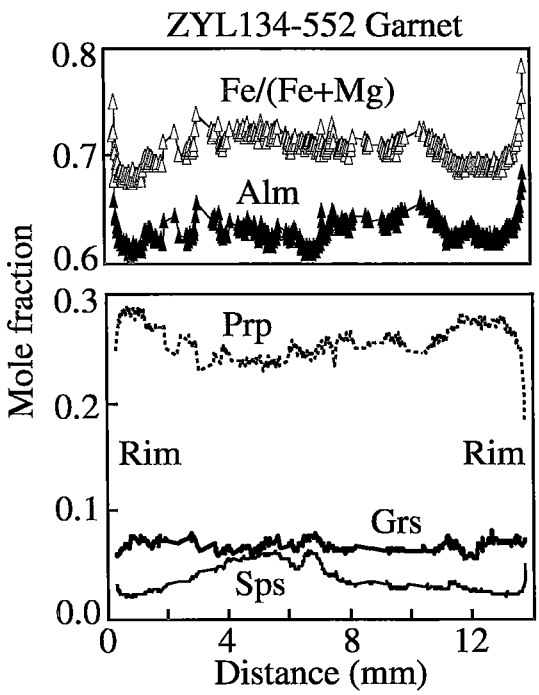

FIG. 13. Compositional zoning of garnet in sample ZYL134–552 along traverse shown in Figure 12 (400 data points).

grains of garnet, but core compositions may have been modified as well at the thermal peak. Garnet compositions with the lowest Fe/(Fe + Mg) 0.8 mm from the rim provide the best available estimate of the compositions at the thermal peak of metamorphism (Spear 1993). Thermometry based on biotite and the near-rim compositions of the garnet gives peak temperatures of 685–700°C (assuming 6 kbar) (Fig. 7). Thermometry based on garnet + amphibole gives similar results (Graham & Powell 1984). Barometry based on the same garnet and biotite, matrix plagioclase and a fictive pure muscovite gives peak conditions of 6.3–6.8 kbar (assuming 700°C), and gives 6.8–7.7 kbar without muscovite. The WebINVEQ approach, using the assemblage garnet + biotite + plagioclase + gedrite, gives dissimilar results, 820°C and 4.5 kbar. In spite of the barometric calculations on this sample, the peak pressure must have been less than 6 kbar, because garnet + cordierite assemblages occur nearby and to the north in the central Kisseynew belt (Bailes & McRitchie 1978). Kraus & Menard (1997) calculated similar peak conditions of 670 °C and 6 kbar for a sample from a similar structural position 3 km to the west. Gordon *et al.* (1994) calculated dissimilar conditions of 580°C and 4.3 kbar for a sample from 45 km northeast of sample ZYL134–552 (and hence not in a similar structural position) and did not claim that these conditions were representative of the peak of metamorphism. Consequently, we prefer 650–700°C and 5–6 kbar as the best estimate of the peak conditions, and explain the discrepancy with our calculations as the result of garnet compositions that were incompletely re-equilibrated at peak conditions or partially reset after the peak of metamorphism. Thus, the peak temperatures are significantly higher than peak temperatures at Snow Lake, although the peak pressures are similar.

The conditions of metamorphism at the end of garnet growth are poorly known, but likely were similar to those at Snow Lake, on the basis of similar relationships of mineral growth to deformational events in similar assemblages in similar rocks. This similarity is most evident between sample ZYL134–513 (above) and the samples from Snow Lake (above). Although the Fe/(Fe + Mg) value of the garnet core is markedly higher in sample ZYL134–552 than in the Snow Lake samples, the rim compositions are similar (Table 2). The differences in composition of garnet core may simply reflect the different peak temperatures of the samples and partial re-equilibration in sample ZYL134–552, and the similarity of rim compositions may reflect similar retrograde temperatures.

On the basis of these similarities, we estimate that the temperatures at the end of garnet growth were likewise similar in both places, *i.e.*, between 530 and 570°C. Compositions from sample ZYL134–552 for the garnet near-rim, An_{58} plagioclase included in the garnet rim, matrix biotite, with an ideal muscovite yield poorly constrained maximum pressures of 5.1–6.3 kbar (assuming 550°C) and 4.7–5.3 kbar without muscovite, as estimates of conditions at the end of garnet growth.

P–T path

Therefore, the pressure at the end of garnet growth for this sample may have been similar (within 1 kbar) to that at Snow Lake. Furthermore, pressure at the end of garnet growth for sample ZYL134–552 may have been similar to the peak pressure. Although there is no evidence for the shape of the path between these two points, the simplest scenario is that heating up to the peak temperatures was nearly isobaric (Fig. 7).

Although compositional zoning of the garnet should not be used in calculating a P–T path because of the possibility of modification by diffusion, a P–T path for the time of garnet growth can be estimated. The following observations place constraints on the P–T trajectory during garnet growth: garnet grew, staurolite was consumed, with increase in the Zn content (0.18 to 0.39 Zn atoms per 48 atoms of oxygen, or 0.04 to 0.08 X_{ZnSt}), and plagioclase was consumed, with decrease in X_{An} (An_{91} to An_{50}). The assemblage garnet +

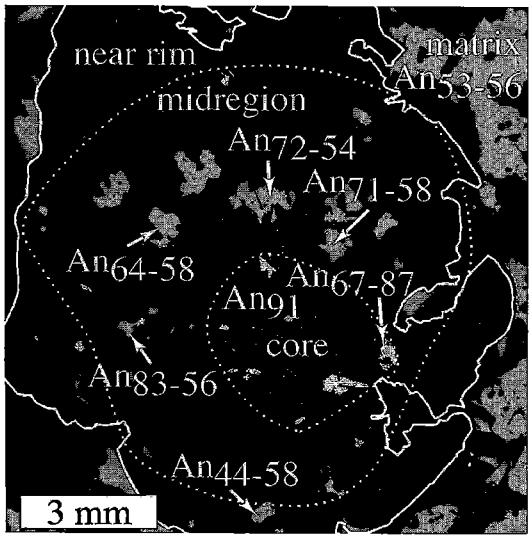

FIG. 14. X-ray compositional map of An content of plagioclase included in garnet in sample ZYL134–552. The heavy white line outlines the grain (*cf.* Fig. 12).

staurolite + biotite + chlorite + plagioclase + quartz + muscovite + H_2O was modeled in a 10-component system (Table 3). The addition of mass-balance constraints (using mineral modes in the calculations) reduces the variance to 2, allowing isopleths to be contoured in P–T space. The composition of chlorite was estimated (Dickenson & Hewitt 1986) with the garnet activity model of Berman (1990), because prograde chlorite was not preserved. Figure 15 shows calculated isopleths of garnet composition and abundance, plagioclase composition (related to plagioclase abundance), and the Zn content of staurolite (inversely related to staurolite abundance). The path that best satisfies the available constraints is a nearly isothermal increase in pressure of 1–2 kbar. Uncertainty in the amount of muscovite does not propagate into a change of the model isopleths. Doubling the amount of chlorite in the model results in an insignificant change in the shape of the isopleths.

SUMMARY OF METAMORPHIC HISTORY

In our collection of samples, metamorphism during the F_1 isoclinal folding event is recorded by a chlorite + quartz or muscovite + quartz schistosity, depending on rock composition. These mineral assemblages suggest that temperatures during F_1 reached 300–400°C (Spear & Cheney 1989). Conditions of metamorphism during F_2 were broadly similar in the samples from Snow Lake and from the Kisseynew gneisses 8 and 16 km to the northeast. Pressure increased during F_2 by 1–2 kbar up to a maximum of *ca.* 5 kbar during minor heating of 10–40°C. The shape of this P–T path is similar to paths characteristic of terranes with nappe- or thrust-style deformation (Spear & Selverstone 1983, Spear 1993). A "nappe- or thrust-style" interpretation for F_2 folds at Snow Lake is consistent with interpretations of Lithoprobe seismic data for the south flank of the Kisseynew Domain (Fig. 2). We conclude that F_2 deformation produced 3–6 km of crustal thickening above samples at the level of the present erosion-surface at Snow Lake, and that the thickening was of similar magnitude across the study area.

The rim of the garnet in some Photo Lake samples (see above) and staurolite porphyroblasts in other samples (unpubl. data) overgrew S_2 and record a minor late heating event of *ca.* 10°C that postdates F_2. In contrast, our samples from the Kisseynew Domain display post-S_2–F_2 heating of 100–150°C. Some heating is expected following overthrusting or emplacement of nappes, simply by relaxation of the perturbed geotherms (England & Thompson 1984, Spear 1993), which explains the minor heating at Photo Lake. The much greater post-F_2 heating in the Kisseynew gneisses, however, requires that there be some additional cause for the heating. Several models are possible to explain the production of a thermal anomaly in the Kisseynew Domain immediately after F_2 shearing, including overthrusting, crustal thinning, emplacement of plutons, or crustal delamination. These models are discussed in the companion paper by Kraus & Menard (1997).

In the Snow Lake area, F_3 is displayed as minor chloritization associated with development of a crenulation cleavage and a locally important fluid-flow event (Menard & Gordon 1995).

ACKNOWLEDGEMENTS

The Hudson Bay Exploration & Development Company and TVX Gold supported this research with grants-in-kind and access to their drill core, geochemical data, and mines. We thank Jurgen Kraus, Al Bailes, and Jerry Kitzler for discussions on the geology of the area, and Steve Lucas for comments on tectonic scenarios. This paper has benefitted from comments by J. Kraus, K. Ansdell, A. Bailes, E. Froese, S. Lucas, M. J. Kohn, and M. St-Onge.

REFERENCES

AGGARWAL, P.K. & NESBITT, B.E. (1987): Pressure and temperature conditions of metamorphism in the vicinity of three massive sulfide deposits, Flin Flon – Snow Lake belt, Manitoba. *Can. J. Earth Sci.* **24**, 2305-2315.

ANSDELL, K.M., KYSER, T.K., STAUFFER, M.R. & EDWARDS, G. (1992): Age and source of detrital zircons from the Missi Formation: a Proterozoic molasse deposit, Trans-Hudson Orogen, Canada. *Can. J. Earth Sci.* **29**, 2583-2594.

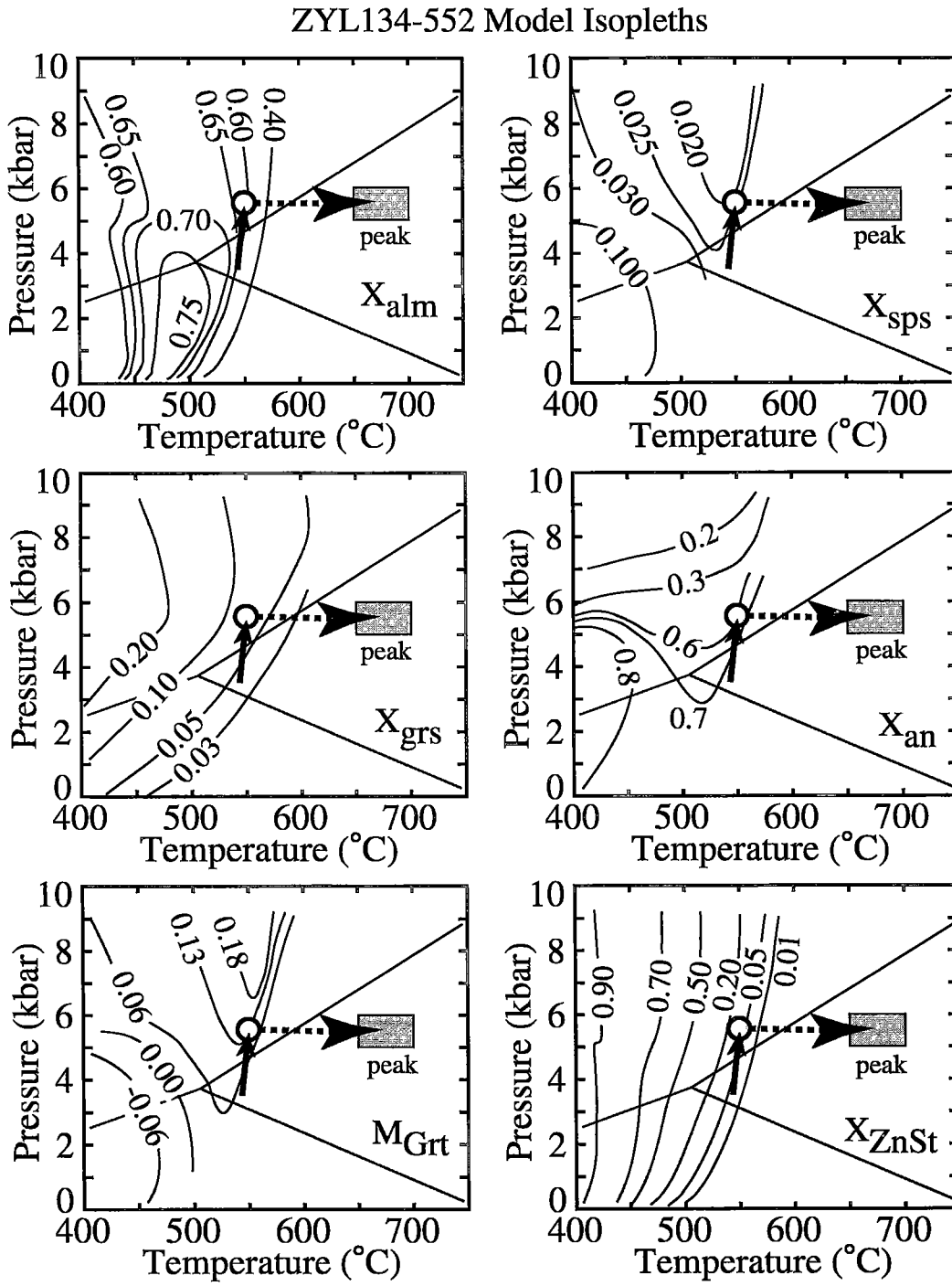

FIG. 15. Model isopleths of compositions of garnet (X_{Alm}, X_{Sps}, X_{Grs}), plagioclase (X_{An}), and Zn in staurolite (X_{ZnSt}), and garnet abundance (M_{Grt}) calculated for sample ZYL134–552. Petrological constraints (see text) suggest an increase of pressure at the time of garnet growth, as shown. The large dot indicates conditions at the end of garnet growth, and the shaded box indicates conditions at the peak of metamorphism. Thus, post-F_2 heating up to the thermal peak (dashed arrow) is interpreted to have been isobaric.

BAILES, A.H. (1988): Chisel – Morgan Lake project. *Manitoba Energy & Mines, Rep. Activities* **1988**, 53-61.

_____ (1992): Wekusko Lake (North) project (NTS 63J/13SW). *Manitoba Energy & Mines, Rep. Activities* **1992**, 56-64.

_____ (1996): Setting of Cu–Zn–Au mineralization at Photo Lake (part of 63K16). *Manitoba Energy & Mines, Rep. Activities* **1996**, 66-74.

_____ & GALLEY, A.G. (1992): Chisel – Anderson – Morgan lakes (NTS 63K/16E); Wekusko Lake (north) NTS 63J/13SW; Anderson – Kormans and Stall lakes (parts of NTS 63K/16SE and 63J/13SW). *Manitoba Energy and Mines, Preliminary Maps* **1992S-1, 2, 3** (1:20 000).

_____ & _____ (1996): Tectonostratigraphic setting of Paleoproterozoic massive sulfide deposits, Snow Lake, Manitoba. *Geol. Assoc. Can. – Mineral. Assoc. Can., Abstr. Program* **21**, A-5.

_____ & MCRITCHIE, W.D. (1978): The transition from low to high grade metamorphism in the Kisseynew sedimentary gneiss belt, Manitoba. *In* Metamorphism in the Canadian Shield (J.A. Fraser & W.W. Heywood, eds.). *Geol. Surv. Can. Pap.* **78-10**, 155-178.

_____ & SIMMS, D. (1994): Implications of an unconformity at the base of the Threehouse Formation, Snow Lake (NTS 63K/16). *Manitoba Energy & Mines, Rep. Activities* **1994**, 85-88.

BERMAN, R.G. (1988): Internally-consistent thermodynamic data for minerals in the system Na_2O – K_2O – CaO – MgO – FeO – Fe_2O_3 – Al_2O_3 – SiO_2 – TiO_2 – H_2O – CO_2. *J. Petrol.* **29**, 445-522.

_____ (1990): Mixing properties of Ca–Mg–Fe–Mn garnets. *Am. Mineral.* **75**, 328-344.

_____ (1991) Thermobarometry using multi-equilibrium calculations: a new technique, with petrological applications. *Can. Mineral.* **29**, 833-855.

_____ & KOZIOL, A.M. (1991) Ternary excess properties of grossular – pyrope – almandine garnets and their influence in geothermobarometry. *Am. Mineral.* **76**, 1223-1231.

BRISTOL, C.C. & FROESE, E. (1989): Highly metamorphosed altered rocks associated with the Osborne Lake volcanogenic massive sulfide deposit, Snow Lake area, Manitoba. *Can. Mineral.* **27**, 593-600.

BRYNDZIA, L.T. & SCOTT, S.D. (1987): Application of chlorite – sulfide oxide equilibria to metamorphosed massive sulfide ores, Snow Lake area, Manitoba. *Econ. Geol.* **82**, 963-970.

DAVID, J., BAILES, A.H. & MACHADO, N. (1996): Evolution of the Snow Lake portion of the Paleoproterozoic Flin Flon and Kisseynew belts, Trans-Hudson Orogen, Manitoba, Canada. *Precambrian Res.* **80**, 107-124.

DICKENSON, M.P. & HEWITT, D. (1986): A garnet – chlorite geothermometer. *Geol. Soc. Am., Abstr. Programs* **18**, 584.

DIGEL, S.G. & GORDON, T.M. (1995): Phase relations in metabasites and pressure – temperature conditions at the prehnite – pumpellyite to greenschist facies transition, Flin Flon, Manitoba, Canada. *In* Low-Grade Metamorphism of Mafic Rocks (P. Schiffman & H.W. Day, eds.). *Geol. Soc. Am., Spec. Pap.* **296**, 67-80.

ENGLAND, P.C. & THOMPSON, A.B. (1984): Pressure – temperature – time paths of regional metamorphism. I. Heat transfer during the evolution of regions of thickened continental crust. *J. Petrol.* **25**, 894-928.

FEDIKOW, M.A.F. & ZIPRICK, D. (1991): The geological setting of the WIM massive sulphide type Cu deposit, Snow Lake area (NTS 63N/1). *Manitoba Energy & Mines, Rep. Activities* **1991**, 41-42.

FERRY, J.M. & SPEAR, F.S. (1978): Experimental calibration of the partitioning of Fe and Mg between biotite and garnet. *Contrib. Mineral. Petrol.* **66**, 113-117.

FROESE, E. & GASPARRINI, E. (1975): Metamorphic zones in the Snow Lake area, Manitoba. *Can. Mineral.* **13**, 162-167.

_____ & MOORE, J.M. (1980): Metamorphism in the Snow Lake area, Manitoba. *Geol. Surv. Can., Pap.* **78-27**.

FUHRMAN, M.L. & LINDSLEY, D.H. (1988) Ternary-feldspar modeling and thermometry. *Am. Mineral.* **73**, 201-215.

GALLEY, A.G., BAILES, A.H. & KITZLER, G. (1993): Geological setting and hydrothermal evolution of the Chisel Lake and North Chisel Zn–Pb–Cu–Ag–Au massive sulfide deposits, Snow Lake, Manitoba. *Explor. Mining Geol.* **2**, 271.

GORDON, T.M. (1989): Thermal evolution of the Kisseynew gneiss belt, Manitoba: metamorphism at an early Proterozoic accretionary margin. *In* Evolution of Metamorphic Belts (J.S. Daly, R.A. Cliff & B.W.D. Yardley, eds.). *Geol. Soc., Spec. Publ.* **43**, 233-243.

_____ (1992): Generalized thermobarometry: solution of the inverse chemical equilibrium problem using data for individual species. *Geochim. Cosmochim. Acta* **56**, 1793-1800.

_____, ARANOVICH, L.Y. & FED'KIN, V.V. (1994): Exploratory data analysis in thermobarometry: an example from the Kisseynew sedimentary gneiss belt, Manitoba, Canada. *Am. Mineral.* **79**, 973-982.

_____, HUNT, P.A., BAILES, A.H. & SYME, E.C. (1990): U–Pb zircon ages from the Flin Flon and Kisseynew belts, Manitoba: chronology of crust formation at an Early Proterozoic accretionary margin. *In* The Early Proterozoic Trans-Hudson Orogen of North America (J.F. Lewry & M.R. Stauffer, eds.). *Geol. Assoc. Can., Spec. Pap.* **37**, 177-199.

GRAHAM, C.M. & POWELL, R. (1984): A garnet – hornblende geothermometer: calibration, testing, and application to

the Pelona Schist, southern California. *J. Metamorphic Geol.* **2**, 13-21.

HAAR, L., GALLAGHER, J. & KELL, G.S. (1979): Thermodynamic properties for fluid water. *In* Water and Steam: their Properties and Current Industrial Applications (J. Straub & K. Scheffler, eds.). *Proc. 9th Int. Conf. Properties Steam.* Pergammon, Oxford, U.K. (69-82).

HAWTHORNE, F.C., UNGARETTI, L., OBERTI, R., CAUCIA, F. & CALLEGARI, A. (1993): The crystal chemistry of staurolite. III. Local order and chemical composition. *Can. Mineral.* **31**, 597-616.

HODGES, D.J. & MANOJLOVIC, P.M. (1993): Application of lithogeochemistry to exploration for deep VMS deposits in high grade metamorphic rocks, Snow Lake, Manitoba. *J. Geochem. Explor.* **48**, 201-224.

HODGES, K.V. & CROWLEY, P.D. (1985): Error estimation and empirical geothermobarometry for pelitic systems. *Am. Mineral.* **70**, 702-709.

HOISCH, T.D. (1990): Empirical calibration of six geobarometers for the mineral assemblage quartz + muscovite + biotite + plagioclase + garnet. *Contrib. Mineral. Petrol.* **104**, 225-234.

HOLDAWAY, M.J., MUKHOPADHYAY, B. & DUTROW, B.L. (1995): Thermodynamic properties of stoichiometric staurolite $H_2Fe_4Al_{18}Si_8O_{48}$ and $H_6Fe_2Al_{18}Si_8O_{48}$. *Am. Mineral.* **80**, 520-533.

HOLLAND, T.J.B. (1989): Dependence of entropy on volume for silicate and oxide minerals: a review and predictive model. *Am. Mineral.* **74**, 5-13.

HUTCHEON, I. (1979): Sulphide – oxide – silicate equilibria: Snow Lake, Manitoba. *Am. J. Sci.* **279**, 643-665.

JUNGWIRTH, T.L. & GORDON, T.M. (1993): Metamorphism in the Duval Lake area (NTS 63N/4). *Manitoba Energy & Mines, Rep. Activities* **1993**, 33.

KLEEMAN, U. & REINHARDT, J. (1994): Garnet – biotite thermometry revisited: the effect of Al^{VI} and Ti in biotite. *Eur. J. Mineral.* **6**, 925-941.

KOHN, M.J. (1993): Uncertainties in differential thermodynamic (Gibbs' method) P–T paths. *Contrib. Mineral. Petrol.* **113**, 24-39.

_____, SPEAR, F.S. & DALZIEL, I.W.D. (1993): Metamorphic P–T paths from Cordiera Darwin, a core complex in Tierra del Fuego, Chile. *J. Petrol.* **34**, 519-542.

KRAUS, J. & MENARD, T. (1997): A thermal gradient at constant pressure during compressional deformation across the southern boundary of the Kisseynew Belt, Trans-Hudson Orogen, Canada. *Can. Mineral.* **35**,

_____ & WILLIAMS, P.F. (1993): Structural studies along the northern margin of the Flin Flon – Snow Lake greenstone belt, Snow Lake. *Manitoba Energy & Mines, Rep. Activities* **1993**, 117-118.

_____ & _____ (1994): Cleavage development and the timing of metamorphism in the File Lake Formation across the Threehouse synform, Snow Lake, Manitoba: a new paradigm. *Lithoprobe Rep.* **38**, 230-237.

_____ & _____ (1995): The tectonometamorphic history of the Snow Lake area, Manitoba, revisited. *Lithoprobe Rep.* **48**, 206-212.

KRETZ, R. (1983): Symbols for rock-forming minerals. *Am. Mineral.* **68**, 277-279.

LUCAS, S.B., WHITE, D., HAJNAL, Z., LEWRY, J., GREEN, A., CLOWES, R., ZWANZIG, H., ASHTON, K., SCHLEDEWITZ, D., STAUFFER, M., NORMAN, A., WILLIAMS, P.F. & SPENCE, G. (1994): Three-dimensional collisional structure of the Trans-Hudson Orogen, Canada. *Tectonophys.* **232**, 161-178.

MACHADO, N. & DAVID, J. (1992): U–Pb geochronology of the Reindeer – Superior transition zone and of the Snow Lake area: preliminary results. *Lithoprobe Rep.* **26**, 40-42.

MÄDER, U.K., PERCIVAL, J.A., & BERMAN, R.G. (1994): Thermobarometry of garnet – clinopyroxene – hornblende granulites from the Kapuskasing structural zone. *Can. J. Earth Sci.* **31**, 1134-1145.

MCMULLIN D., BERMAN R.G. & GREENWOOD H.J. (1991): Calibration of the SGAM thermobarometer for pelitic rocks using data from phase-equilibrium experiments and natural assemblages. *Can. Mineral.* **29**, 889-908.

MENARD, T. & GORDON, T.M. (1995): Syntectonic alteration of the VMS deposits, Snow Lake, Manitoba. *Manitoba Energy & Mines, Rep. Activities* **1995**, 164-167.

_____ & SPEAR, F.S. (1993): Metamorphism of calcic pelitic schists, Strafford Dome, Vermont: compositional zoning and reaction history. *J. Petrol.* **34**, 977-1005.

_____ & _____ (1994): Metamorphic P–T paths from calcic pelitic schists from the Strafford Dome, Vermont, U.S.A. *J. Metamorphic Geol.* **12**, 811-826.

NEWTON, R.C., CHARLU, T.V. & KLEPPA, O.J. (1980): Thermochemistry of the high structural state plagioclases. *Geochim. Cosmochim. Acta* **44**, 933-941.

PARENT, M., MACHADO, N. & ZWANZIG, H.V. (1995): Timing of metamorphism and deformation in the Jungle Lake area, southern Kisseynew belt, Manitoba: evidence from U–Pb geochronology of monazite and zircon. *Lithoprobe Rep.* **48**, 131-132.

POWELL, R. & HOLLAND, T.J.B. (1988): An internally consistent dataset with uncertainties and correlations. 3. Applications to geobarometry, worked examples and a computer program. *J. Metamorphic Geol.* **6**, 173-204.

ROBIE, R.A, HEMINGWAY, B.S. & FISHER, J.R. (1979): Thermodynamic properties of minerals and related substances at 298.15 K and 1 bar (10^5 Pascals) pressure and at higher temperatures. *U.S. Geol. Surv., Bull.* **1452.**

SLACK, J.F. (1997a): Extreme metasomatism of basalt at the Elizabeth copper mine, Vermont, U.S.A. – Seafloor hydrothermal vs. regional metamorphic effects. *In* F.M. Vokes Symposium on the Formation and Metamorphism of Massive Sulphide Deposits (Trondheim, Norway). *Abstr. Vol.*, 26

_____ (1997b): The timing and direction of metamorphic fluid flow in Vermont: discussion. *Contrib. Mineral. Petrol.* (in press).

SPEAR, F.S. (1993): *Metamorphic Phase Equilibria and Pressure – Temperature – Time Paths.* Mineral. Soc. Am., Monogr. **1**.

_____ & CHENEY, J.T. (1989): A petrogenetic grid for pelitic schists in the system $SiO_2 - Al_2O_3 - FeO - MgO - K_2O - H_2O$. *Contrib. Mineral. Petrol.* **101**, 149-164.

_____, KOHN, M.J., FLORENCE, F.P. & MENARD, T. (1990): A model for garnet and plagioclase growth in pelitic schist: implications for thermobarometry and P–T path determinations. *J. Metamorphic Geol.* **8**, 683-696.

_____, PEACOCK, S.M., KOHN, M.J., FLORENCE, F.P. & MENARD, T. (1991): Computer programs for petrologic P–T–t path calculations. *Am. Mineral.* **76**, 2009-2012.

_____ & SELVERSTONE, J. (1983): Quantitative P–T paths from zoned minerals: theory and tectonic applications. *Contrib. Mineral. Petrol.* **83**, 348-357.

STERN, R.A., SYME, E.C., BAILES, A.H. & LUCAS, S.B. (1995): Paleoproterozoic (1.9–1.86 Ga) arc volcanism in the Flin Flon belt, Trans-Hudson Orogen, Canada. *Contrib. Mineral. Petrol.* **119**, 117-141.

TREMBATH, G.D. (1986): *The Compositional Variation of Staurolite in the Area of the Anderson Mine, Snow Lake, Manitoba, Canada.* M.Sc. thesis, Univ. of Manitoba, Winnipeg, Manitoba.

ZALESKI, E., FROESE, E. & GORDON, T.M. (1991): Metamorphic petrology of Fe–Zn–Mg–Al alteration at the Linda volcanogenic massive sulfide deposit, Snow Lake, Manitoba. *Can. Mineral.* **29**, 995-1017.

Received November 10, 1996, revised manuscript accepted July 16, 1997.